Russian Chemical Reviews **74** (5) 413 – 441 (2005) © 2005 Russian Academy of Sciences and Turpion Ltd

DOI 10.1070/RC2005v074n05ABEH000886

Chemical vapour deposition of thin-film dielectrics

V Yu Vasilev, S M Repinsky

Contents

I.	Introduction	413
II.	Chemical vapour deposition of thin-film dielectric materials: general	414
III.	Characteristics of film growth processes	417
IV.	Deposition of silicon nitride films	422
V.	Deposition of silicon oxynitride films	426
VI.	Deposition of silicon dioxide films	427
VII.	Deposition of multicomponent silicate glass thin films	436
VIII.	Conclusion	439

Abstract. Data on the chemical vapour deposition of thin-film dielectrics based on silicon nitride, silicon oxynitride and silicon dioxide and on phosphorus- and boron-containing silicate glasses are generalised. The equipment and layer deposition procedures are described. Attention is focussed on the analysis and discussion of the deposition kinetics and on the kinetic models for film growth. The film growth processes are characterised and data on the key physicochemical properties of thin-film covalent dielectric materials are given. The bibliography includes 139 references.

I. Introduction

Layered semiconductor, dielectric and metallic composite materials are used in high-precision technologies. Such structures are the basis of modern electronics (in particular, solid-state integrated circuits are fabricated from single-crystalline silicon on semiconductor wafers).

Fabrication and use of multilayer structures became possible after solving the complicated problems of semiconductor materials science concerned with the synthesis of defect-free dielectric films (*e.g.*, silicon dioxide, silicon nitride, boron nitride and tin, titanium, aluminum, *etc.*, oxide films). At present, such films are fabricated using various versions of the chemical vapour deposition (CVD) technique.[1]

CVD methods have been used to fabricate 'wafer – thin film' structures since the mid-1960s.[2, 3] The growth of a thin film, in the course of a CVD process, on the surface of a wafer heated to the desired temperature is the result of irreversible reactions of initially gaseous compounds. Dielectric films are synthesised using both research and industrial CVD flow reactors operating at atmospheric, reduced and low pressures. Vapour-phase mixtures of the precursors, oxidants or ammonia, in the presence of various carrier gases, are supplied to the reactor by a pressure drop in the carrier gas stream or as a result of the evacuation of the system with a vacuum pump. One of the most important features of CVD processes is the possibility to grow films of variable thickness (from a few hundredths of a micrometre to a few micrometres) at relatively low temperatures. For instance, silicon dioxide films can be CVD grown at temperatures below 373 K, whereas silicon dioxide is formed at a noticeable rate by the oxidation of monocrystalline silicon with O_2 at temperatures above 1173 K. The film synthesis temperature can also be reduced by an additional (non-thermal) activation of the vapour phase using a high-frequency discharge, photochemically or by using laser irradiation.

Wide use of CVD methods in basic research and large-scale production is due to the fact that they require relatively simple equipment, are safe and manufacturable and provide high quality thin-film coatings fabricated under the optimum synthesis conditions. At present, thin-film CVD processes are basic technological processes in electronics [4 – 6] and their proportion in the overall device fabrication cycle is continuously increasing as the devices and methods of fabrication of multilayer structures become more and more complicated.

Both research practice and applied use of CVD methods face the problem of describing the film growth processes, which involves the establishment of some functional dependences.

First, it is necessary to obtain quantitative relations between the film growth rate and the parameters of the CVD process, *e.g.*, temperature (T), pressure (P), linear rate of gas stream (v) and the ratio of the component concentrations in the vapour phase (taking into account the geometry of the CVD reactor), features of the spatial arrangement of wafers in the reactor and the thermal and gas-dynamic effects in the reactor. Usually, these are the key factors for the optimization of the film deposition process, which eventually involves achievement of a maximum film growth rate at a minimum possible film thickness mismatch (desired values lie within limits of a few percent) across the entire wafer surface.

There are a number of good examples of solving optimization problems in film growth processes for different reactor types and various dielectric materials. One of them is modelling the operation of a low-pressure flow tube reactor under isothermal conditions.[7] The authors [7] succeeded in determining the parameters and spatial arrangement of wafers corresponding to a minimum film thickness mismatch at maximum reactor charge (several tens or even hundreds of semiconductor wafers). This is, in particular, due to the fact that no detailed information on the chemical stages of the growth process was required; the model

V Yu Vasilev, S M Repinsky Institute of Semiconductor Physics, Siberian Branch of the Russian Academy of Sciences, prosp. Acad. Lavrent'eva 13, 630090 Novosibirsk, Russian Federation. Fax (7-3832) 33 27 71, tel. (7-3832) 30 85 91, e-mail: vladislav_v_2000@yahoo.com (V Yu Vasilev), repinsky@land.ru (S M Repinsky)

Received 26 November 2003
Uspekhi Khimii **74** (5) 452 – 483 (2005); translated by A M Raevskiy

included only the rate constants for the reactions on the wafer surface or in the vapour-phase and the vapour-phase diffusion coefficients. However, in spite of the paramount importance of this solution, it is only a particular case for modelling of CVD process.

The second necessary functional dependence is a relation between the chemical composition and microcomposition of the film and the input parameters of the CVD process. For instance, the composition of silicon nitride films grown by ammonolysis of monosilane is usually described by the formula Si_3N_4. However, the microcomposition of such films should be described in terms of concentrations of the NH and SiH groups,[8] because the overall concentration of hydrogen in the silicon nitride films can vary between 4 at.% and 20 at.%, depending on the CVD method employed in each particular case. For many practical applications in electronics, the microcomposition plays the key role; therefore, this level of modelling of the CVD process requires knowledge of all stages of the growth process.

The third group of functional dependences includes correlations between the properties of the deposited films and the CVD conditions. It should be noted that most studies of the properties of dielectric materials were carried out using a particular deposition technique and a narrow range of parameters for the CVD processes.

Finally, searching for correlations between the electrophysical properties of deposited materials and the CVD parameters, including the reactor type, starting compounds, deposition conditions, *etc*., is also an important task.

The considerable interest in the CVD processes is reflected in a continuous stream of publications, most of which describe the operation regimes, reactors and the properties of the films obtained. The properties of the films have been studied to different extents. Silicon-based films widely used in electronics have been best studied. The results of the investigations of silicon nitride films obtained up to 1980 have been comprehensively treated in a monograph.[8] Data on the deposition of silicon dioxide films, and especially binary and ternary silicate glass films, have almost not been summarised earlier. More complex thin-film materials, *e.g*., silicate glasses, synthesised in four- and five-component chemical systems, have been poorly studied. This leads to an inadequate understanding of the physicochemical processes used in electronics. This conclusion can be drawn after close examination of the available monographs.[2–6] For instance, at present, the epitaxy, diffusion and thermal oxidation processes have been studied in detail and theoretically substantiated, whereas chemical vapour deposition of dielectric thin films is still descriptive in character.

This review is concerned with the analysis of the problems of CVD of dielectric thin films. We discuss the methodological problems of CVD and the fundamentals of the molecular theory of dielectric film growth. The key characteristics responsible for the growth processes and main physicochemical properties of thin-film covalent dielectric materials are also considered.

II. Chemical vapour deposition of thin-film dielectric materials: general

1. Reactions

Basic to CVD processes are the following chemical reactions of carbon and silicon compounds: pyrolysis (cracking process), reduction, oxidation, hydrolysis, ammonolysis and dehydrogenation. Given below are some examples of these reactions.

Pyrolysis

$$Ni(CO)_4 \longrightarrow Ni + 4CO,$$

$$SiH_4 \longrightarrow Si + 2H_2,$$

$$Si(OC_2H_5)_4 \longrightarrow SiO_2 + 4C_2H_4 + 2H_2O.$$

Reduction

$$SiCl_4 + 2H_2 \longrightarrow Si + 4HCl,$$

$$WF_6 + 3H_2 \longrightarrow W + 6HF.$$

Oxidation

$$SiH_4 + O_2 \longrightarrow SiO_2 + 2H_2,$$

$$4PH_3 + 5O_2 \longrightarrow 2P_2O_5 + 6H_2,$$

$$2B_2H_6 + 3O_2 \longrightarrow 2B_2O_3 + 6H_2,$$

$$SiH_4 + 4N_2O \longrightarrow SiO_2 + 2H_2O + 4N_2,$$

$$SiH_2Cl_2 + 2N_2O \longrightarrow SiO_2 + 2N_2 + 2HCl.$$

Hydrolysis

$$TiCl_4 + 2H_2O \longrightarrow TiO_2 + 4HCl,$$

$$SiF_4 + 2H_2O \longrightarrow SiO_2 + 4HF.$$

Ammonolysis

$$3SiH_4 + 4NH_3 \longrightarrow Si_3N_4 + 12H_2,$$

$$3SiH_2Cl_2 + 10NH_3 \longrightarrow Si_3N_4 + 6NH_4Cl + 6H_2,$$

$$3SiCl_4 + 16NH_3 \longrightarrow Si_3N_4 + 12NH_4Cl,$$

$$B_2H_6 + 2NH_3 \longrightarrow 2BN + 6H_2.$$

Interaction with methane

$$SiCl_4 + CH_4 \longrightarrow SiC + 4HCl.$$

Interaction with monosilane

$$2MoCl_5 + 4SiH_4 \longrightarrow 2MoSi_2 + 10HCl + 3H_2.$$

Among these, the hydrolysis and oxidation reactions are the fastest. A special position is occupied by the oxidation of silane, which proceeds as a branched-chain process; therefore, SiO_2 films can be fabricated at low temperatures ($\sim$343 K). Note that in the case of CVD processes, the reaction schemes presented above can be used for descriptive purposes only, because the composition of the by-products depends on the particular conditions. For instance, the oxidation of hydrides under CVD conditions can result in both hydrogen and water.

Studies on the deposition of silicon nitride films in the course of the interaction between $SiCl_4$ and NH_3, and of nickel films during pyrolysis of nickel carbonyls, were carried out more than four decades ago. Since then, some concepts of the character of these processes have been proposed and accepted.[8,9] The CVD approach can be employed to obtain (i) dielectric materials (SiO_2, binary and ternary glasses $SiO_2-B_2O_3$, $SiO_2-P_2O_5$, $SiO_2-B_2O_3-P_2O_5$, Si_3N_4, silicon oxynitride $Si_3N_4-SiO_2$ and Al_2O_3, AlN, Ge_3N_4, TiO_2, TiC, TiN), which are used as screening films, protective coatings, mirrors and waveguides; (ii) polycrystalline and amorphous semiconductor films (silicon, SiC and compounds of the types $A^{III}B^{V}$ and $A^{II}B^{VI}$) used for fabrication of transistor structures; (iii) metals and alloys (Ni, Al, W, Ta and Mo and nickel, manganese, iron, titanium, cobalt, chromium, tungsten, tantalum, molybdenum, platinum and aluminum silicides) for production of conductors; (iv) superconductors Nb_3Sn, Nb_3Ge, $YBa_2Cu_3O_{7-x}$, $Bi_2Sr_2Ca_{n-1}Cu_nO_x$ ($n = 1-3$); (v) ferroelectrics $Pb(Zr,Ti)O_3$ and $(Ba,Sr)TiO_3$; (vi) transparent conductors $SnO_2(In_2O_3)$, *etc*.

Thin film–wafer composites have found a variety of technological applications in electronics, mechanical engineering, power engineering, medicine, *etc*. The CVD method differs from other known thin film fabrication techniques (thermal, plasma or ion deposition) in the size of the deposited particles, which is of the order of a few tenths of a nanometre (*cf*. tens of nanometres for other methods). Molecular dispersion of the deposited particles makes possible the deposition of compact coatings on surfaces

with complex reliefs, with good adhesion and high mechanical properties for the coatings.

2. Thermodynamic aspects of CVD

The problem of growth of a dielectric film is part of the known problem with solid phase formation from particles present in gas or vapour phases. The thermodynamic aspect of this problem was first considered by Volmer.[10] The cases for complex multicomponent systems used for epitaxial crystal growth were generalised by Schäfer[11] and Kuznetsov *et al.*[12] However, it is impossible to analyse the film growth rate using thermodynamic description of chemical systems, because the vast majority of dielectric film fabrication processes proceed under conditions that are far from the thermodynamic equilibrium.

Concerning the possibility of using the crystal-growth theory methods to describe the growth of dielectric thin films, we can say the following.

The modern crystal-growth theory concerns three main problems:

— the mechanism of a new phase nucleation on the surface of a crystal or in the medium surrounding the growing crystal (*e.g.*, the gas or vapour phase);

— the nature of the processes that govern the nucleation kinetics (according to the layer-by-layer growth theory, these are the surface diffusion processes);

— the problem of retention of the growing plane in the crystal; solutions to this problem are best demonstrated in the Kossel model for an ideal crystal and in the model by Frank, Burton and Cabrera[13] for a real crystal (motion of the front of a screw dislocation).

In the theory of gas-phase nucleation, the critical radius, r_c, of a spherical nucleus is expressed through the surface energy σ; the molecular volume, υ_m, of the nucleus; the vapour pressure P_v; and the equilibrium pressure P_e at the temperature T

$$r_c = \frac{2\sigma\upsilon_m}{RT\ln(P_v/P_e)}. \quad (1)$$

Consider, as an example, formation of silicon dioxide films by the oxidation of monosilane with O_2, assuming that the gas–solid system is in thermodynamic equilibrium. Using the following dependence,†

$$P_e = 4.11 \times 10^{13} \exp\left(-\frac{336.4}{RT}\right)$$

we obtain $P_e = 4 \times 10^{-8}$ Pa for $T = 573$ K. Then, using the published data[14,15] for $P_e = 133.3$ Pa ($\upsilon_m = 22$ cm^3 and $\sigma = 2 \times 10^{-5}$ J cm^{-2}), we get $r_c = 0.03$ nm. This means that the formation of silicon dioxide film does not begin with a homogeneous nucleation step. However, it is known that (i) reactions of monosilane with oxygen-containing oxidants (O_2, N_2O, CO) result in SiO_2 as the solid product and (ii) silicon dioxide molecules transferred to the vapour phase upon evaporation of this compound are present only above molten SiO_2 (at $T \sim 2273$ K).[14] Therefore, chemical vapour deposition of silicon dioxide films proceeds under conditions that are far from the thermodynamic equilibrium. Similar analysis of the growth of silicon nitride films in the course of monosilane ammonolysis leads to the same conclusion.

The analysis given above excludes the possibility of forming three-dimensional nuclei in the vapour phase; however, we can assume the appearance of a two-dimensional nucleus on the surface and consider the unique kinetic features of its growth. The melting temperatures, T_m (in K), of silicon and silicon compounds and the temperature intervals (ΔT) corresponding to typical conditions of synthesis for these compounds are listed below.

† From this point on the activation energy is given in kJ mol^{-1}.

Material	T_m	$(2/3)T_m$	ΔT
Silicon	1693	1128	870–910
Silicon dioxide	1773	1182	470–970
Silicon nitride	2173	1448	970–1120

It is known that atom transfer processes, such as diffusion, viscous flow, recrystalisation, *etc.*, can be considered fast if they proceed at temperatures exceeding a value of $(2/3)T_m$. The data listed above show that in all cases silicon dioxide and silicon nitride films are formed at temperatures that are several hundreds of degrees lower than the corresponding $(2/3)T_m$ value. This means that the mobility of the atoms of the growing film is hindered in the course of synthesis and the surface self-diffusion cannot be as intense as is assumed in layer-by-layer crystal growth theory.

Quantitative information about surface diffusion can be extracted from the results of experiments on the sintering of finely dispersed SiO_2 powders obtained by hydrolysis of organosilicon compounds. The activation energy for the sintering of powders is known to be nearly 711 kJ mol^{-1}; this process only proceeds at a measurable rate at 1273 K.[16]

Thus, thin-film dielectric materials are formed under CVD conditions as a result of complex heterogeneous chemical reactions involving vapour-phase processes and transformations on the growing surface of the dielectric material.

3. Kinetic aspects of CVD. Multipath and multistage film growth processes

Thin-film dielectric materials can be fabricated by deposition from vapour phases containing at least two reactive components using three main types of reactions. These are pyrolysis (thermal decomposition of organoelement compounds), oxidation and ammonolysis. For instance, SiO_2 films can be obtained under CVD conditions and by pyrolysis, while Si_3N_4 films can be prepared by ammonolysis of silicon compounds.

Let us illustrate specific features of the kinetics of the CVD reaction by taking silicon nitride films obtained in two reactions, (1) $SiCl_4 + NH_3$ and (2) $SiH_4 + NH_3$, as examples. For the reaction involving $SiCl_4$, the formation of a product of direct interaction, $Cl_3SiNH_2^+$, in the vapour phase was detected by mass spectrometry,[17] the concentration of $Cl_3SiNH_2^+$ being about 20% of the starting concentration of the $SiCl_3^+$ ion. Considerable amounts of products of secondary collisions, containing one or two silicon atoms and NH_2 groups were also detected; besides, these products always contain HCl. These results show that the first intermediate product of the vapour-phase reaction is Cl_3SiNH_2 and further reactions result in the formation of $Si(NH_2)_2Cl_2$ and Si_2NHCl_6 particles. Detained analysis of these reaction schemes and information on the rate constants for the different stages can be found in the literature (see, *e.g.*, Refs 8, 18, 19). Figure 1 presents a scheme of possible transformations of the starting reagents in the formation of Si_3N_4 films.

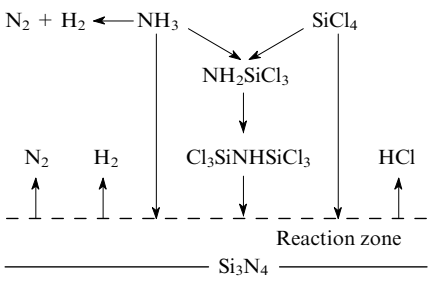


Figure 1. A scheme illustrating the sequence of stages and routes of chemical transformations during the formation of silicon nitride layers in the $SiCl_4$–NH_3 system.[18]

In the $SiH_4 + NH_3$ system, the sequence of reactions, resulting in the formation of silicon nitride films, can involve both pure vapour-phase reactions:

$$2\,NH_3 \rightleftharpoons N_2 + 3\,H_2,$$

$$SiH_4 \rightleftharpoons SiH_2 + H_2,$$

$$SiH_2 + SiH_4 \longrightarrow Si_2H_6,$$

$$Si_2H_6 \longrightarrow 2\,SiH_3,$$

$$n\,Si_2H_6 \longrightarrow (SiH_2)_{2n} + n\,H_2,$$

and surface reactions:

$$2\,NH_3 \rightleftharpoons 2\,N_{(ads)} + 3\,H_2,$$

$$NH_3 \rightleftharpoons N_{(ads)} + 3\,H_{(ads)},$$

$$2\,NH_3 \rightleftharpoons 2\,NH_{3(ads)} \longrightarrow N_{2(gas)} + 3\,H_{2(gas)},$$

$$SiH_4 \longrightarrow SiH_{4(ads)},$$

$$SiH_2 \longrightarrow SiH_{2(ads)},$$

$$SiH_3 \longrightarrow SiH_{3(ads)},$$

$$SiN_{3/3}NH_2 \longrightarrow SiN_{4/3} + H_2,$$

$$2\,NSi_{2/4}SiH_3 \longrightarrow 2\,NSi_{3/4} + 3\,H_2.$$

These reaction schemes serve as the basis for a generalised kinetic model of a complex CVD reaction, determining the growth of a film. For instance, the overall reaction of the precursors A and B (Fig. 2) results in the formation of structural units of a thin-film dielectric material (DM)

$$A + B = DM.$$

This reaction is generally a multistage and multipath process. Consider three main paths. Route I is the interaction between A and B in the adsorption layer by the Langmuir–Hinshelwood or by the Eley–Rideal mechanisms. Route II is the interaction between the intermediate product, I, and the surface, *S*, of the growing film, resulting in the formation of an intermediate product, F, which is eventually transformed in the reaction zone into structural units of the DM and thus causes regeneration of an element of the pristine surface. Route III is characterised by the formation of the intermediate product, I, in the vapour phase and the subsequent formation of a by-product (end product C).

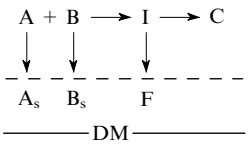


Figure 2. Generalised kinetic scheme of formation of a dielectric layer during the CVD process.[18]
A and B are the starting reagents; A_s and B_s are the reagents in the adsorption state; I and F are intermediate products in the vapour phase and in the adsorption layer, respectively; C is a side product (gas or powder); and DM is the end product (thin layer of dielectric material).

The aforementioned can be represented as the matrix of stoichiometric coefficients of CVD stages (Table 1). In this representation, the growth process is described as a complex reaction following three concurrent routes, each of them being a multistage process. In particular, route I involves stages *2*, *3*, *4* and *6*; route II involves stages *1*, *5* and *6* and route III involves stages *1* and *7*. Thus, the growth of a dielectric thin film can be considered as a multipath and multistage chemical reaction. To describe the kinetics of this reaction, one must have a complete set of rate constants for each of the individual stages. This is an intricate experimental task, which importantly can be solved using the formal approaches developed in the theory of the kinetics of heterogeneous catalysis.

Table 1. Matrix of stoichiometric coefficients of different stages of the CVD process.[18]

No.	Stage	Route		
		I	II	III
1	A + B = I	0	1	1
2	$A + S = A_s$	1	0	0
3	$B + S = B_s$	1	0	0
4	$A_s + B_s = F$	1	0	0
5	I + S = F	0	1	0
6	F = DM	1	1	0
7	I = C	0	0	1

4. Structural aspect of thin film synthesis under CVD conditions

Formation of thin-film dielectric materials under CVD conditions proceeds as a heterogeneous chemical reaction , *i.e.*, a sequence of elementary acts involving the embedding of structural units into the matrix of the growing film. An important feature of this class of compounds is the absence of long-range order in their structures. Short-range order in covalent dielectric materials can be described using the concept of structural units proposed by Myuller.[20] A structural unit is the smallest possible atomic group in the nearest coordination sphere of a given atom, which reflects its coordination and the unique features of its embedding into the matrix material. Examples of the main structural units are provided by $SiO_{4/2}$ for silicon dioxide, $BO_{3/2}$ and $BO_{4/2}$ for boron oxide, $O^-P^+O_{3/2}$ for phosphorus oxide, $GeO_{4/2}$ for germanium oxide and $SiN_{4/3}$ for silicon nitride. The properties of a layer can strongly depend, not only on the main unit, but also on other structural units. For instance, SiO_2 layers can contain inclusions with $\equiv Si-OH$ or $\equiv Si-H$ bonds, *i.e.*, structural units $SiO_{3/2}OH$, $SiO_{2/2}(OH)_2$ or $HSiO_{3/2}$, $H_2SiO_{2/2}$. This means that the layer compositions should be described as sets of structural units responsible for the short-range order in the layer of dielectric material. Another important feature is connected with the character of a given combination of structural units, which governs the nature of the medium-range order in the layer. It is known that the $SiO_{4/2}$ tetrahedra in SiO_2 layers can be combined in such a fashion that formations of four-, five-, six- and eight-membered rings, comprised of the $Si-O-Si$ bridges, become possible. This results in the appearance of micropores and mesopores in the matrix.

Structural features of synthesised films are also related to the character of the long-range order in the structure. When synthesising semiconductor films, it is usually possible to obtain single-crystalline films. Metal films are, as a rule, polycrystalline, while the synthesis of dielectric materials leads to formation of glassy or amorphous films. Interrelations between these structures are illustrated in Fig. 3, which shows variations in the structure of a SiO_2 film of various degrees of disorder.[21]

The key role in the formation of a film structure is played by the temperature of the wafer, but generally one must also take into account other starting parameters of the CVD processes. Note that the properties of the surface of a dielectric material are determined by the set of the surface structural units characterised by the different heats of adsorption of the reagents. In this connection, one can assume a non-uniform energy distribution across the surface of the growing dielectric material. In contrast to the crystal model by Kossel, in which non-uniform energy distribution is determined by structural features, the model of a growing dielectric film is governed by the discrete set of structural units with different chemical compositions. This can be exemplified by considering the data on the surface chemistry of silica gels and quartz glass.

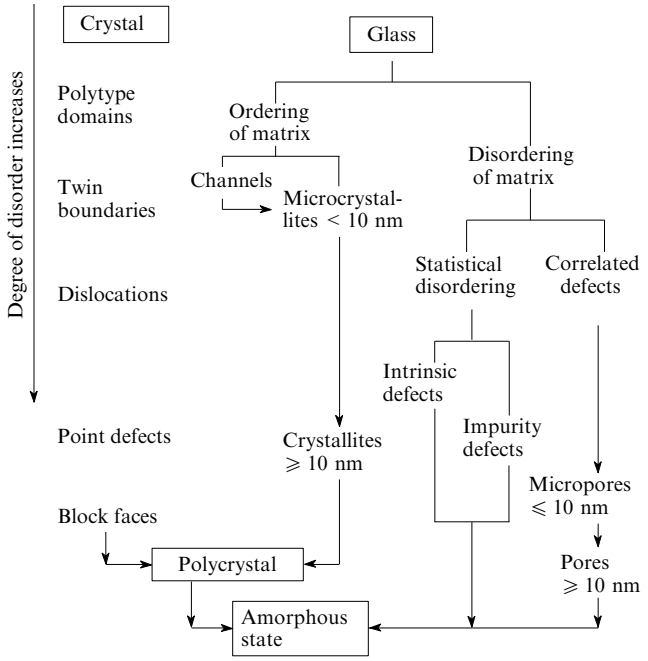


Figure 3. Scheme illustrating interrelations between defects in the crystalline, glassy and amorphous silicon dioxide.[21]

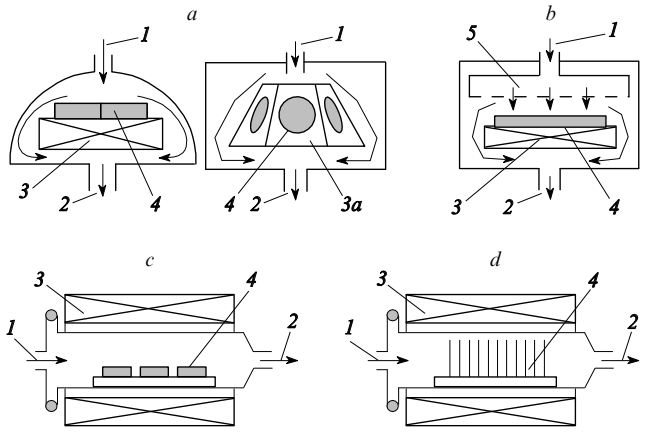


Figure 4. Main types of reactors (simplified schemes): atmospheric pressure reactor (*a*), reduced pressure reactor (*b*), low pressure reactor (*c*) and low pressure reactor with cross-vertical coaxial arrangement of wafers (*d*).
Gas inlet (*1*), exhaustion of used gas mixture or evacuation (*2*), heater (*3*), pyramidal heater (*3a*), wafer (*4*), gas distributor system (including the system with high-frequency power) (*5*).

A study of the surface of a cleaved SiO_2 face revealed the presence of $O_2SiO_{3/2}$ and $OSiO_{3/2}$ sites (see Ref. 22). Investigations of the adsorption characteristics of silica gels [23, 24] established the presence of the $(O_{3/2}Si)_2O$, $HOSiO_{3/2}$ and $(HO)_2SiO_{2/2}$ surface sites. The results of studies of the growth of polycrystalline silicon films and the data on hydrogen adsorption on the surface of this material indicates the formation of the $HSiSi_{3/4}$ and $H_2SiSi_{2/4}$ surface sites. Thus, generally, the surface energy of the growing dielectric material can be different at different points of the surface, owing to the chemical inhomogeneity of the adsorption sites. However, it should be noted that this can manifest itself only at low coverages of the adsorption layer. If the growth occurs as a monolayer or ultrahigh coverage, the kinetics of the process should be described with allowance for uniform energy distribution across the surface.

In the theory of layer-by-layer crystal growth, an important role is played by screw dislocations, whose outcrops provide a kind of constant sink for adatoms to the monatomic step. A distinctive feature of the glassy state of a compound is the absence of regular dislocation-type defects. This means that structurally, a dielectric film has a highly ordered surface. Some problems can be due to crystallisation of films, *viz*., if it does occur, structural defects appear on the surface of the dielectric film.

It is possible to analyse various growth processes of thin-film dielectric materials from a unified point of view by using the concept of a reaction zone (a concept traditionally used in solid state chemistry when considering topochemical reactions). In certain simple cases, the reaction zone can be as thin as the monolayer coating. Generally, the thickness of the reaction zone is in the order of a few atomic sizes.

III. Characteristics of film growth processes

1. CVD equipment and reagents

A number of simplified schemes of flow reactors most widely used for the deposition of dielectric films are shown in Fig. 4. In these reactors, wafers can be arranged on heated pedestals or inside a quartz tube with isothermal heating. In the former case, the temperature of the reactor walls is lower than the wafer temperature; these reactors being called 'cold-wall' reactors. In the latter case, wafers and reactor walls have the same temperature; these reactors being called 'hot-wall' reactors. The spatial arrangement of wafers in 'hot-wall' reactors can vary, namely, along or normal to the gas stream (see Fig. 4 *c*,*d*); respectively, one deals with flow and flow-diffusion reactors.

Depending on the reagent pressure, CVD reactors are conditionally divided into the atmospheric pressure reactors ($P \geqslant 1 \times 10^5$ Pa), reduced pressure reactors ($P < 1 \times 10^5$ Pa) and low pressure reactors ($P \sim 10-2000$ Pa). The abbreviations of the corresponding CVD processes, derived from the reactor names, are APCVD, RPCVD and LPCVD, respectively. As the pressure under CVD conditions decreases, the reagent diffusion coefficients increase and the process is shifted to such an operation regime for which the mass transfer conditions become insignificant. This makes it possible to vary the spatial orientation of wafers, and hence improve the performance of CVD processes in the flow-diffusion LPCVD reactors (see Fig. 4 *d*).

The gas flow rate in the course of deposition can vary from a few (LPCVD reactors) to several hundreds (APCVD reactors) of $cm^3\ s^{-1}$, which approximately corresponds to a range of linear rates for the gas stream from a few cm s^{-1} (APCVD reactors) to tens of m s^{-1} (LPCVD reactors). Evacuation of LPCVD reactors is achieved using high-pressure vacuum pumps. If necessary, so-called Roots pumps are also used; their performance can be as high as several hundreds of $dm^3\ s^{-1}$, at pressures ranging between a few tens to hundreds of Pa.

A significant drawback of all flow reactors is their low performance due to incomplete consumption (often, less than 10%) of the starting reagents, which often does not meet environmental safety conditions. Studies on the possibility of using reactors with a closed gas cycle for the synthesis of thin films led to unsatisfactory results, owing to intense formation of by-products (microparticles) in the cold regions of reactors. However, it was found that silicon nitride films can be synthesised from $SiCl_4$ and NH_3 using a LPCVD reactor with a quasi-closed cycle. After evacuation of the reactor, the flow rates of the starting reagents, in the ratios corresponding to the stoichiometric equation, are specified. A stable low pressure in the reactor is self-maintained during the course of the growth process, because all products of this reaction are isolated as solids deposited on the cold walls of the reaction chamber.

Thin film deposition itself occurs when the vapour–gas mixture of a specified composition is supplied for a necessary

time interval into the reactor containing no atmospheric gases (this is achieved by blowing-in an inert gas or by evacuation); the wafer temperature must be pre-stabilised. Equipment and methods for the deposition of thin-film dielectric materials have been well documented (see, *e.g.*, Refs 25–27).

Numerous combinations of various compounds were used in the studies of the CVD synthesis of dielectric films carried out over a long period of time. For instance, silicon dielectric films were deposited using monosilane, disilane, dichlorosilane, silicon tetrachloride, tetraethylorthosilicate (TEOS), dimethyldichlorosilane, hexamethyldisilazane and hexamethyldisiloxane. Nowadays, the starting combinations of silicon compounds for industrial use in electronics are well established.

Silicon nitride films are mainly synthesised by ammonolysis of dichlorosilane in LPCVD reactors and much more rarely by ammonolysis of silicon tetrachloride. The ammonolysis of monosilane is mainly used in the case of plasma-enhanced deposition.

Silicon dioxide films, as well as boron-containing and phosphorus-containing glass films are fabricated using two versions of the CVD method:

— hydride technique involving monosilane (if necessary, phosphine and diborane are also used) and oxygen in all types of reactors at a low temperature ($\sim$673 K); in some cases, boron trichloride and organic esters of boric, phosphorous or phosphoric acids are used instead of diborane and phosphine;

— pyrolysis of tetraethylorthosilicate at temperatures above 923 K or oxidation of mixtures of this compound with organic esters in all types of reactors at a low temperature ($\sim$673 K); here, possible oxidants are oxygen or oxygen–ozone mixtures (with ozone concentration of up to 13 mass%).

2. Characteristics of film deposition regimes in flow reactors

Gas flows under CVD conditions are characterised by the Reynolds number

$$\mathrm{Re} = \frac{\rho_g \upsilon d}{\eta_g}$$

(ρ_g is the density of the gas, η_g is the viscosity of the gas, υ is the linear flow rate of the gas stream and d is the characteristic linear size of the reactor), which varies between 10 and 100. At such Re values, turbulence effects are insignificant. Depending on the total pressure in the reactor, the Knudsen numbers (ratio of the mean free path of molecules to the linear size of the reactor) vary from 1 (in RPCVD reactors) to 10^{-4} (in APCVD reactors). If a process is carried out at a pressure in the range 133–1333 Pa, the diffusion coefficients of reagents increase by 1.9–2.9 orders of magnitude compared to their values under normal conditions. Because of this, the process becomes kinetically controlled. A quantitative characteristic of this regime is the ratio of the reaction rate to the diffusion rate — the Thiele criterion, which, for a first-order reaction, has the form

$$\Phi = \frac{kd}{D},$$

where k is the rate constant for the reaction and D is the diffusion coefficient. At $\Phi \leqslant 0.1$, the process is determined by the rate of the heterogeneous reaction, becoming diffusion controlled at $\Phi \geqslant 1$.

3. Experimental determination of film growth rate constants

Methodologically correct determination of the growth rate constants is of crucial importance for the qualitative description of film growth processes under CVD conditions. The growth rate depends on specific features of the heat and mass transfer processes, *viz.*, the reactor and wafer heating mode, reactor geometry, shape of wafer pedestals, reactant gas supply technique, total pressure and linear flow rates of gas mixtures. In some particular cases, it is possible to perform quantitative heat and mass transfer calculations and determine the growth rate constants. These parameters can also be determined experimentally.

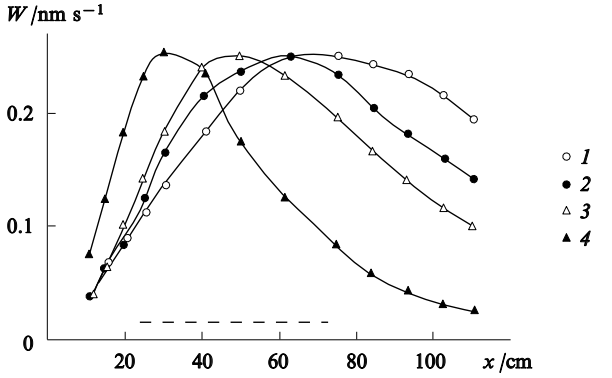


Figure 5. Growth rate distribution of silicon nitride layers along the axis of a horizontal isothermal reactor with isothermal zone 1123 K (shown by dashed line).[8]
Linear rate /cm s^{-1}: 494 (*1*), 395 (*2*), 328 (*3*) and 197 (*4*); P = 1995 Pa, $[SiH_4] = 2.76 \times 10^{-7}$ mol $litre^{-1}$, $[NH_3]/[SiH_4] = 90$.

Isothermal horizontal tube reactors of internal radius r_r = 20–60 mm (see Fig. 4*c*,*d*) with a sufficiently extended isothermal zone in the central part of the reactor appear to be most convenient for carrying out such experiments. The length of the isothermal zone is usually at least one third of the total length of the reactor. The thickness of the film deposited on wafers (wafer radius, r_w, usually lies between 20 and 50 mm) varies along the length of the reactor, namely, it increases at the beginning of the isothermal zone, reaches a maximum value and decreases near the end of the isothermal zone. This is illustrated in Fig. 5. In the initial portions of curves, the deposition rate (W) increases to its maximum value (W_{max}), corresponding to the instant when the gas stream is heated in the whole volume. Subsequent decrease in the deposition rate is due to depletion of monosilane. Let a gas stream move along the reactor at the linear rate υ and the gas mixture arrives at point x at time

$$\tau = \frac{x}{\upsilon},$$

which is called the residence time of the gas mixture in the reactor. Using this ratio, the dependence of the rate of the process on the coordinate (along the reactor) can be re-calculated to the corresponding dependence on τ.

After this treatment, the family of dependences shown in Fig. 5, plotted in the new coordinates, looks as a single kinetic curve, passing through a maximum (τ_{max}). In this case, the process can be described by the model of a plug reactor, which is based on two assumptions: (1) constant reagent concentrations at a given reactor section and (2) the rate of convective transfer of a reagent is higher than the diffusion rate along the reactor axis. Analysis of the curves plotted in Fig. 6*a* revealed yet another salient feature, namely, depletion of the gas mixture decreases exponentially (this is clearly seen in Fig. 6*b*).

The rate of conversion of the ith component, of initial concentration c_{0i}, in the course of a first-order chemical reaction is expressed as follows:

$$-\frac{\mathrm{d}c_i}{\mathrm{d}t} = kc_i,\ c_i = c_{0i}\exp(-kt).$$

From here, the rate constant for the reaction is given by:

$$k = \frac{\Delta \ln(c_i/c_{0i})}{\Delta t}.$$

The rate constant for the reaction can be determined by plotting the film growth rates, W_{max}, corresponding to maxima on the $W(x)$ curves (see Fig. 5) *vs.* concentration c_{0i}:

$$W_{\max} = kc_{0i}^{n}.$$

In this case, it is possible to determine both the rate constant k and the reaction order n. Determination of the initial concentration c_{0i} can appear to be difficult. In the case in point, the stage described by the raising portion of the $W(\tau)$ curve (see Fig. 6 *a*) is characterised by partial depletion of the gas mixture from the ith component, and the c_{0i} value does not correspond to the real initial concentration. The depletion value, Δc_i, must be calculated by integrating the total mass of the layer formed on the reactor walls from the point corresponding to the beginning of registration of the film growth to the point $x_{\max}$ (maximum position):

$$\Delta c_i = \xi \frac{\rho_f 2\pi r_r}{\upsilon_T M} \int_0^{x_{\max}} W_x \mathrm{d}x.$$

Here ξ is the stoichiometric number, which shows how many moles of the ith reagent should be consumed in order to form 1 mole of product, ρ_f is the film density, υ_T is the gas flow rate at the temperature T and M is the molecular mass of the film material. This expression for Δc_i is valid for a cylindrical reactor with horizontally arranged small wafers (see Fig. 4 *c*). In other cases (*e.g.*, vertically arranged wafers), calculations are more complicated.

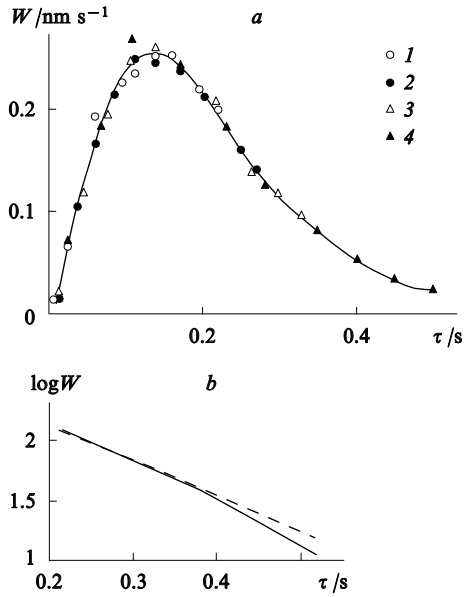


Figure 6. Dependences presented in Fig. 5 plotted in the 'growth rate–residence time of the gas mixture in the reactor' coordinates (*a*) and in semilogarithmic coordinates (*b*).[8]
For notation (*1–4*), see the caption to Fig. 5.

If the change, Δh, in the thickness of the deposited film after time Δt in a flow reactor of the surface area S equals the deposition rate W_s, one can find the number, Δm, of moles of reaction product formed:

$$\Delta m = \frac{S\rho_f}{M}\frac{\Delta h}{\Delta t}\Delta t = \frac{S\rho_f}{M} W_s \Delta t.$$

For a static system or under plug reactor conditions one has

$$\Delta m = -\xi V \frac{\Delta c}{\Delta t}\Delta t = -\xi V W_v \Delta t,$$

where V is the volume of the reactor, c is the molar concentration of the reagent and W_v is the rate of the vapour-phase reaction. For a one-path process, one gets a simple relation between these rates:

$$\frac{\mathrm{d}h}{\mathrm{d}t} = \xi \frac{VM}{S\rho_f}\frac{\mathrm{d}c}{\mathrm{d}t}.$$

Generally (the case of multipath reactions), $W_v > W_s$ and the ratio of these rates determines the contribution of a given path. When the reaction kinetics is studied experimentally, one must determine how the ratio of the surface area, S, of the reactor to its volume, V, affects the reaction rate. This criterion allows us to answer the question of which (gas-phase or heterogeneous) stage is the rate-determining step of the reaction. Assuming that a certain reaction is characterised by the dependence $W = kc$, if the overall rate is determined by the slow surface reaction, *i.e.*,

$$W_s = \frac{\mathrm{d}h}{\mathrm{d}t} = k_s c,$$

where k_s is the rate constant for the surface reaction, the rate of the reagent conversion is given by

$$-\frac{\mathrm{d}c}{\mathrm{d}t} = \frac{S\rho_f}{M\xi V}\frac{\mathrm{d}h}{\mathrm{d}t}$$

and

$$\frac{\mathrm{d}c}{c} = \frac{S\rho_f}{M\xi V} k_s \mathrm{d}t.$$

From here it is seen that:

$$W_s = k_s c_0 \exp\left(-\frac{S}{V}\frac{\rho_f}{M\xi}k_s t\right).$$

Having determined the rate constant at $t = 0$ (this corresponds to the position in the plot shown in Fig. 6 *a*), we obtain the k_s value, which is independent of the reactor geometry. Using the experimental data in the $\ln W - t$ coordinates, one can find the effective rate constant

$$k = \frac{S}{V}\frac{\rho_f}{M\xi}k_s,$$

which depends on the S/V ratio. In particular, for cylindrical reactors one has $S/V = 2/r_r$. In this case it is convenient to compare the reaction development times τ_1 and τ_2, corresponding to the same degree of reagent conversion in reactors of different cross-sectional areas (radii r_{r1} and r_{r2}). As can be seen, $\tau_1/\tau_2 = r_{r1}/r_{r2}$. This can be illustrated by Fig. 7, where the growth rate of silicon nitride films in the reaction of monosilane with ammonia in different cylindrical reactors is plotted against time. Both cases are characterised by the same maximum rate, although the linear gas flow rates differ by nearly a factor of four. Assuming that the reactions are complete at, *e.g.*, 70% conversion, one can obtain $\tau_1 = 0.26$ and $\tau_2 = 0.10$ s, the τ_1/τ_2 ratio being in good agreement with the ratio $r_{r1}/r_{r2} = 38/16 = 2.4$.

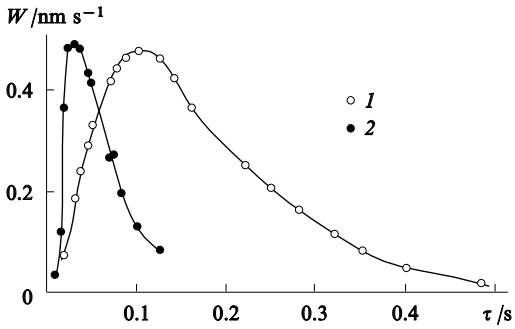


Figure 7. Growth rate of silicon nitride layer plotted *vs.* the residence time of gas mixture in reactors of radii 38 (*1*) and 16 mm (*2*).[8]
$T = 1123$ K, $P = 2000$ Pa, $[SiH_4] = 3.64 \times 10^{-7}$ mol litre^{-1}, gas flow rate 70 cm^3 s^{-1} under normal conditions, $[NH_3]/[SiH_4] = 90$.

Let us consider a volume gas-phase reaction. Assuming that passage of the gas containing an active reagent with the concentration c along the reactor at the rate v_T results in the formation of a film of thickness Δh after time Δt:

$$\Delta h = \frac{M}{S\rho_F} v_T c \Delta t .$$

The rate constant for the deposition reaction is given by:

$$k = \frac{M\xi}{S\rho_F} v_T .$$

From here we get:

$$W = \frac{M}{S\rho_F} v_T c_0 \exp\left(-\frac{Mxi}{S\rho_F} v_T t\right).$$

This equation shows that, firstly, the deposition rate at $t = 0$ is proportional to the linear gas flow rates. Secondly, a decrease in the reaction rate with time, in reactors of different cross-sections and experiments with constant linear gas flow rate, is independent of the reactor cross-section and inversely proportional to the reactor surface area (for a cylinder, to $\sim r_r^{-1}$) at constant gas flow rate.

Mention may also be made that the rate constants for growth can be most reliably determined when using the dependences that follow the process to high degrees of reagent conversion. Usually, the progression of the reaction is accompanied by significant changes in the kinetics of the process and, as a consequence, by changes in the properties of the growing film. Processes in LPCVD reactors are conducted to low degrees of reagent conversion (usually, 5% – 10%); therefore, such reactions are of limited use for determining rate constants.

4. Comparative characteristics of industrial CVD processes

Practical implementation of CVD in high-precision technologies often involves the use of various reactors and various combinations of reagents (and hence chemical reactions) with significantly different deposition conditions. In addition, different CVD processes are described to different extents. In particular, the approach to the determination of the rate constants (see above) has only been practically implemented for silicon nitride. Numerous studies on the subject report mainly on the dependences of the deposition rates on some parameters of the CVD processes for particular types of reactors, while the geometric parameters of reactors are often not reported.

However, long-term investigations in the field of the synthesis of silicon-based dielectric materials showed that different film deposition processes can be compared, in order to determine the most efficient technology, by using simplified approaches that are consistent with the general method of analysis of the rate constants (see above). The good reasons are as follows.

Firstly, the kinetic dependences shown in Fig. 5, as an example, appeared to be valid for all dielectric thin film deposition processes involving two or more components. The dependences only differed in the positions of the maxima of curves (the exceptions are pyrolysis of monosilane and oxidative pyrolysis of TEOS). In addition, the reactors studied met the ideal displacement conditions.

Secondly, almost all dielectric film deposition processes studied are first order with respect to the silicon-containing compound and pseudo zero order with respect to oxidants or ammonia. Acceleration or retardation of the oxidation processes in the presence of phosphorus or boron compounds manifested themselves in corresponding changes in the film growth rates.

Thirdly, industrial CVD processes proceed under conditions of maximum reaction yield, which correspond to regions of maxima in the kinetic curves.

Fourthly, modern deposition processes are performed at similar S/V ratios because high-quality film deposition in reactors requires elimination of the 'extra' volumes in which undesired gas-phase processes can proceed. For instance, the spacing between wafers in the most widely used industrial CVD reactors (see Fig. 4 *b*,*d*) is ~ 5 mm.

Fifthly, using the film growth laws, industrial CVD processes can be characterised by a simplified approach to multipath and multistage reactions. In the framework of the kinetic model discussed above, we chose a simplified model for a CVD process, which involves three possible paths: a heterogeneous route (I), a two-stage route involving stages of homogeneous formation and heterogeneous consumption of the intermediate product (II) or formation of side aerosol products (III).

To perform a generalised characterisation of CVD processes, the main parameter chosen was the so-called effective rate constant, k_{ef}, for the process, *i.e.*, the ratio of the deposition rate, corresponding to the maximum value (W_{max}) in the $W = f(\tau)$ curve, to the concentration of the silicon component [Si] in the vapour phase

$$k_{ef} = \chi \frac{W_{max}}{[Si]}, \qquad (2)$$

where χ is the coefficient of proportionality. Substantiation of this approach to the description of CVD processes and the determination of k_{ef} is available in the literature (see, *e.g.*, Refs 28 – 31). A comparison of different processes for the synthesis of polycrystalline silicon, silicon nitride and silicon dioxide thin films and glasses showed that the experimental k_{ef} value lies in the range $\sim 0.3 - 10$ cm s^{-1}.

Based on the results obtained, a classification of CVD processes for silicon thin films was proposed,[29-31] which allows for the specific features of the thin film synthesis in various chemical systems (Table 2).

5. Growth of thin film dielectrics on relief surfaces

Fabrication of high-precision microelectronic devices involves a transformation of an initially planar wafer surface into a relief surface. The width of gaps separating adjacent elements of devices and the relief height can vary from fractions of a micrometre to a few micrometres. Film deposition on relief surfaces occurs at different rates. This fact is allowed for by so-called layer conformality,[4-6] *i.e.*, the ratio of the film thickness on the lateral face of the step to the film thickness on the top of the step h_2/h_1 (Fig. 8). It was established [29, 32, 33] that layer conformality (in %) in the dielectric silicon film deposition processes depends on the rate constant k_{ef}; the approximate empirical relation being as follows:

$$\frac{h_2}{h_1} \approx 45.4 k_{ef}^{-0.51}.$$

Some experimentally determined conformality values and intervals for the deposition on relief steps of rectangular cross-section are listed in Table 2.

Thin film deposition on the relief steps of microelectronic devices comprising ultra-small gaps between elements faces the

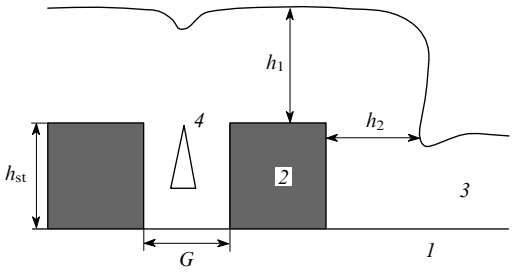


Figure 8. Cross-section of steps with deposited layer and corresponding main parameters.[33]
Wafer (*1*), relief step (*2*), deposited layer (*3*) and unfilled void (*4*).

Table 2. Classification of CVD processes of silicon-containing thin films.[30–32]

Process characteristics	Type of CVD process					
	A	B	C	D	E	F
Chemical system		SiH_4 (pyrolysis) →			SiH_4-PH_3; SiH_4-NH_3; $SiH_4-O_2(-PH_3)$	fast non-optimised oxidation and ammonolysis reactions involving SiH_4 including PE-CVD [a] of silicon nitride and silicon dioxide
		→		SiH_4-N_2O (< 950 K) →	SiH_4-N_2O (> 950 K)	
			$SiH_2Cl_2-NH_3$; $SiCl_4-NH_3$; $SiH_2Cl_2-N_2O$	$(CH_3)_2SiCl_2-O_2$ →	$(CH_3)_2SiCl_2-O_2-PCl_3$	
		→			$(C_2H_5O)_4Si-O_2-PH_3$	
		$(C_2H_5O)_4Si$ (pyrolysis) →	$(C_2H_5O)_4Si-O_2-B(OC_3H_7)_3$			
		→			$(C_2H_5O)_4Si-O_3/O_2-PO(OCH_3)_3$, and optimised PE-CVD of silicon nitride and silicon dioxide	
	$(C_2H_5O)_4Si-O_3/O_2$ →		$(C_2H_5O)_4Si-O_3/O_2-B(OC_2H_5)_3$			
k_{ef} /cm s^{-1}	0.1 – 0.2	< 2.7 [b] ~ 0.38 [c]	0.05 – 0.28	0.12 – 1.0	~ 0.37 [d] 1 – 2.6 [e]	> 2
Factors responsible for constant film thickness	CVD conditions	CVD conditions	CVD conditions	CVD conditions and reactor design	reactor design	–
Minimum film thickness non-uniformity (%)	< 2	< 2	< 2	< 5	< 10	> 10
Aerosol formation	no	no	no	no	no	yes
Layer conformality (%)	~ 130	~ 100	90 – 100	70 – 90	40 – 70	0 – 20
Reaction route, possible limiting stage	I	I	II, consumption of intermediate product on wafer	II	II, formation of intermediate product in the vapour phase	II and III, formation of intermediate product in the vapour phase
Performance of CVD process for cylindrical LPCVD (see Fig. 4 *d*), number of wafers used in the process		250	200	80	50	–

Note. Arrows denote which types correspond to a particular initial CVD process (groups A, B C) characterised by retardation or acceleration of the deposition reaction upon variation of temperature, addition of the second reagent (in pyrolysis) and addition of boron and phosphorus compounds (in oxidation processes). Analysis was performed based on the k_{ef} values taking into account (i) dependences of the film thickness non-uniformity on the parameters of the CVD process and on the reactor design, (ii) data on non-uniform thin-film deposition on the relief surfaces (see below), *etc*. The averaged values of the maximum performance of CVD processes (at the minimum film thickness non-uniformity values listed in this Table) for the most widely used cylindrical low-pressure flow CVD reactors are given in the bottom line.

[a] PE-CVD is Plasma-Enhanced CVD. [b] For pyrolysis of SiH_4. [c] For pyrolysis of $(C_2H_5O)_4Si$. [d] For the joint pyrolysis of SiH_4 and PH_3. [e] For the oxidation and ammonolysis reactions.

problem of high-quality (continuous) filling of the gaps with deposited film containing voids (see Fig. 8). This problem is known in the literature as the 'Gap fill' problem. A possible criterion for the filling of a certain gap is the parameter h_{st}/G^2 (Refs 32 and 33). The quality of gap filling using CVD methods can be assessed using the approximate relationship:

$$\frac{h_{st}}{G^2} \approx 3.03 k_{ef}^{-1.47}$$

(h_{st}/G^2 in μm^{-1}).

6. Modern approaches to the optimisation of industrial CVD processes

The modern high-precision technologies used in microelectronics were designed to be implemented in so-called group production, *i.e.*, treatment of a particular number of wafers during one technological process. This approach implies a very high level (>95%) of reproducibility of the properties of the material and the sizes of device elements within the same semiconductor wafer, and for all wafers within the same group. This requires (i) determination of the most important parameters of the CVD processes under study, which can influence the device characteristics, and (ii) plotting their distributions schematically, shown in, *e.g.*, Fig. 9 *a*. The desired reproducibility of the parameters of high-precision devices is achieved as a result of the optimisation of technological processes, which implies a search for an optimum 'parameter window' for the CVD process (see Fig. 9 *b*), which can be realised in a reactor by using a particular combination of starting reagents. In the case of CVD processes, the number of such parameters is rather large, *viz.*, the temperature, reagent concentrations, pressure, reagent feed rate, *etc.*

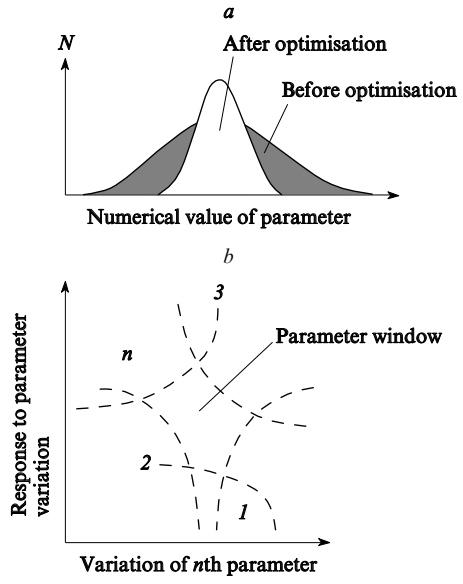


Figure 9. Conditional CVD parameter distribution before and after optimisation of the deposition process (*a*) and the parameter window (*b*). Dashed lines correspond to parameters *1*–*n*.

Optimisation leads to a narrowing of the parameter distribution (see Fig. 9 *a*). A CVD process reproducibility in the chosen parameter window is confirmed by running the 'marathon' test (check of the equipment and technological processes for continuous operation, or the mean-time-between-failure evaluation). When running such tests, the total number of wafers treated in a 24 h day can be as high as a few thousands, all film parameters being checked for, *e.g.*, on every 25th wafer. The reproducibility control of the CVD process, and maintenance of the parameter distribution within the specified intervals and within the limits of necessary deviations, is achieved using methods of mathematical statistics. Combining this approach with full automation of the film deposition equipment allows one to obtain reproducible film thickness parameters and the physicochemical and electrophysical properties of the films deposited.

IV. Deposition of silicon nitride films

Silicon nitride and boron nitride thin film fabrication technology is based on the ammonolysis reactions at elevated temperatures in the vapour phase. Silicon nitride deposition reactions are conducted using silicon hydrides, silicon halides, ammonia and hydrazine.[8]

The results of kinetic studies of SiH_4 and $SiCl_4$ ammonolysis have been summarised.[8,34] Only a few publications concerned with the kinetics of dichlorosilane ammonolysis are available, and these data have not been reviewed so far. Below we present the most important data on the kinetics and growth mechanisms of the systems involving SiH_4, $SiCl_4$, SiH_2Cl_2 and NH_3.

1. System SiH_4 – NH_3

The main kinetic characteristics of the process of silicon nitride film deposition in the temperature range 873–1123 K were determined using an isothermal reactor, operating in the ideal-displacement regime at linear gas flow rates ranging between 4 and 20 cm s^{-1}. These characteristics depend on the monosilane concentration (in the range from 1×10^{-5} to 7×10^{-5} mol $litre^{-1}$) and ammonia concentration (in the range from 2×10^{-5} to 2.5×10^{-2} mol $litre^{-1}$). The film growth rate increases in proportion to the increase in the monosilane concentration; the activation energy for this reaction, equal to 160.6 kJ mol^{-1}, was determined from the temperature dependence of the rate constant. The reaction rate is independent of the ammonia concentration in the range from 1×10^{-5} to 1×10^{-3} mol $litre^{-1}$ and then monotonically increases. Taken altogether, the kinetic data obtained were described by the following empirical equation:[8]

$$W = k_1[SiH_4]\left[\frac{k_2[NH_3]}{1+k_2[NH_3]} + (1.80 \pm 0.05)\right]\frac{1}{1+k_3[H_2]}. \quad (3)$$

The coefficients of this equation are listed in Table 3. The k_1 constants of the processes carried out at reduced pressures are five to ten times higher than those carried out at atmospheric pressure. The difference is more pronounced when comparing the data for processes performed at higher temperatures. One can assume that the more accurate k_1 values were determined in the experiments at a reduced pressure. This permits the most accurate determination of the rates at low degrees of monosilane conversion (here, the content of such a reaction product as, *e.g.*, hydrogen in the vapour phase, can be neglected).

To analyse the reaction of monosilane with ammonia, let us return to Fig. 5, which presents the silicon nitride growth rate distribution along the isothermal zone of the reactor. The decrease in the monosilane concentration during the reaction corresponds

Table 3. Parameters of empirical equation (3) obtained for the low and atmospheric pressure CVD reactors (Å litre mol^{-1} min^{-1}).[8]

T/K	k_1		k_2	k_3
	LPCVD	APCVD		
873	–	0.58×10^6	–	–
973	$(10.6\pm1.6)\times10^7$	0.81×10^7	0.26×10^4	0.49×10^3
1023	$(4.9\pm0.6)\times10^8$	–	–	–
1073	$(6.7\pm0.7)\times10^8$	0.33×10^8	0.11×10^4	0.31×10^3
1123	$(10.6\pm0.2)\times10^8$	–	–	–

to 30% – 50% monosilane conversion. At these degrees of conversion, the monosilane decomposition rate is given by:[35]

$$\frac{d[H_2]}{dt} = 10^{13.2} \exp\left(-\frac{214.0}{RT}\right)[SiH_4] .$$

Unfortunately, this equation is valid for a relatively narrow temperature range. But the assumption of its validity at $T = 973$ K is such that, if the overall reaction is limited by the rate of the homogeneous reaction, these degrees of conversion will be attained at a distance of a few millimetres from the beginning of the isothermal zone. These estimations suggest that thermal decomposition of monosilane, considered as a stage of the synthesis of silicon nitride, is a fast reaction. The reactions

$$SiH_4 \rightleftharpoons SiH_2 + H_2 ,$$

$$SiH_2 + SiH_4 \longrightarrow Si_2H_6 ,$$

$$Si_2H_6 \longrightarrow 2\,SiH_3$$

result in the formation of the vapour-phase species SiH_2 and SiH_3, involved in the interaction with the solid surface:

$$SiH_2 \longrightarrow SiH_{y(sol)} + \left(\frac{1-y}{2}\right)H_2 ,$$

$$SiH_3 \longrightarrow SiH_{y(sol)} + \left(\frac{3-y}{2}\right)H_2 .$$

The composition of the particles forming the solid phase varies depending on the degree of monosilane conversion. Tetravalent silicon in $SiH_{y(sol)}$ is involved in Si – H bonding and in the bonds with the atoms of the solid phase (Si – Si or Si – N). At $y = 2$, the surface SiH_2 group is not an adsorption site, but at $y < 2$ it can form a chemisorption bond. Hydrogen desorption from silicon surfaces has been well studied [36, 37] and it was shown that hydrogen atoms are strongly adsorbed on the silicon surface and that an exposure of 0.3 Langmuir leads to the formation of coatings similar to monolayers. Two adsorption forms can be clearly seen in the thermodesorption spectra. It is assumed that the first form corresponds to the surface complex $\equiv SiH$, characterised by a desorption energy of 2.5 ± 0.1 eV; the second form being the structure $=SiH_2$, with a desorption energy of 1.9 ± 0.3 eV.

Thermal decomposition of ammonia in the vapour phase at low pressures is proportional to the ammonia and inert gas concentrations, the rate constant (in s^{-1}) being given by: [38]

$$k = 10^{14.4} \exp\left(-\frac{275.8}{RT}\right).$$

In studies of the thermal decomposition of ammonia in ammonia–argon mixtures at Ar concentrations in the range $6 \times 10^{-4} - 3 \times 10^{-3}$ mol cm^{-3}, the first order rate constant (in s^{-1}) is found from the equation:

$$k = 10^{12.82 \pm 0.54} \exp\left(-\frac{409.6 \pm 20.9}{RT}\right).$$

The reaction proceeding under these conditions involves breaking of the N – H bond, characterised by a dissociation energy of 427.3 kJ mol^{-1}.

Vapour-phase synthesis produces no stable intermediates (SiH_4 and NH_3). A laser IR heating study [39] of the pyrolysis of monosilane – ammonia mixtures revealed (i) almost no decrease in the ammonia concentration under conditions of fast monosilane decomposition and (ii) the absence of stable products of the reaction between monosilane and ammonia, in the vapour phase. However, in the presence of ammonia the activation energy for monosilane pyrolysis decreases from 250.4 ± 8.4 to 154.2 ± 8.4 kJ mol^{-1}. No simple explanation for this effect has been proposed as yet. One can assume that the reaction between ammonia and monosilane results in unstable products, which favours generation of radicals. One such product can be silylamine H_2NSiH_3. In contrast to similar phosphorus and arsenic compounds, H_2PSiH_3 and H_2AsSiH_3, silylamine is unstable; attempts at detecting it in the vapour phase having failed.

Thus, vapour-phase decomposition of ammonia can occur only at temperatures that are much higher than the temperature interval under study, 873 – 1073 K. Therefore, the decomposition of ammonia mainly proceeds by a heterogeneous mechanism, described by the following reactions:

$$NH_3 \rightleftharpoons NH_{3(ads)} , \qquad (4)$$

$$NH_{3(ads)} \longrightarrow \gtrdot NH_{(ads)} + H_{2(gas)} .$$

As can be seen, the surface of the growing silicon nitride film meets the conditions necessary for establishment of an adsorption equilibrium. For instance, conventional film growth rates lie in the range $10^{-2} - 10^{-1}$ nm s^{-1} (*i.e.*, $\sim 5 \times 10^{14}$ molecule cm^{-2} s^{-1}). The collision frequency of NH_3 molecules with the surface is 3×10^{16} molecule cm^{-2} s^{-1} at a partial pressure of 1330 Pa, being a few orders of magnitude higher than the growth rate. Therefore, reaction (4) results in the establishment of an equilibrium, which is followed by a concentration dependence of the process, according to the Langmuir equation. The effective heat of adsorption of ammonia on the silicon nitride surface is 95.3 kJ mol^{-1}.

Decomposition of monosilane and ammonia leads to the formation of groups containing Si – H or N – H bonds on the film surface. The presence of chemisorbed hydrogen atoms on the surface hampers further adsorption; because of this, reactions producing active sites (hydrogen desorption reactions) are needed:

$$SiH_{2(ads)} \longrightarrow Si_{Si_3N_4} + H_{2(gas)} ,$$

$$\gtrdot NH_{(ads)} \longrightarrow N_{Si_3N_4} + \frac{1}{2}H_{2(gas)} .$$

The retarding effect of hydrogen in the temperature range 973 – 1073 K at $[SiH_4] = 3.0 \times 10^{-5}$ and $[NH_3] = 6.4 \times 10^{-3}$ mol $litre^{-1}$ manifests itself as a dramatic decrease in the deposition rate [40] upon changing the hydrogen concentration from 0 to 3.5×10^2 mol $litre^{-1}$. The effective heat of hydrogen adsorption on the silicon nitride surface, determined from the temperature dependence of the adsorption constant, is 67.3 kJ mol^{-1}. Yet another reason for the retardation of the synthesis of silicon nitride in the presence of hydrogen can be the reversibility of the vapour-phase reaction, *e.g.*,

$$SiH_4 \rightleftharpoons SiH_2 + H_2 . \qquad (5)$$

In this case

$$[SiH_2] = \frac{[SiH_4]}{[H_2]}K,$$

where K is the equilibrium constant.

Based on the natural assumption that the reaction rate is proportional to the concentration of SiH_2 particles, we summise that the temperature dependence of the reaction rate must have the form $\exp[-(E_a + \Delta H)/RT]$, where E_a is the activation energy for the reaction proceeding in the absence of hydrogen in the vapour phase, and ΔH is the enthalpy of the reaction of SiH_2 production from monosilane. The enthalpies of formation of monosilane and silylene are 34.6 and 247.9 kJ mol^{-1}, respectively;[41] therefore, the effective activation energy for the reaction must increase by 213.3 kJ mol^{-1} in the presence of hydrogen. It was experimentally found that the activation energy for the deposition of silicon nitride films in the presence of hydrogen is 234 kJ mol^{-1}, *i.e.*, increases by $\sim 66 - 75$ kJ mol^{-1}. Hence, our assumption of shift of the equilibrium in a certain vapour-phase reaction in the presence of hydrogen contradicts the experimental data.

Thus, the growth rate of silicon nitride films in the reaction of monosilane with ammonia is determined by a transformation in the adsorption layer, hydrogen desorption being the slowest stage. The results of our qualitative considerations permit the derivation of an expression for the growth rate of dielectric films. Let us

assume that four types of adsorption site can be present on the surface of a growing silicon nitride film. These types are as follows: **I** — $>$Si, **II** — $>$SiH$_2$, **III** — $>$Si(NH$_3$)$_{(ads)}$ and **IV** — $>$SiNH.

Assume also that only one reaction, *e.g.*, reaction (5), can proceed in the vapour phase. Consider the following reactions involving the adsorption sites on the surface of the growing film:

$$>\!\text{Si:} + \text{SiH}_4 \xrightarrow{k_1} >\!\text{Si}\cdot\text{SiH}_2 + \text{H}_2,$$

$$>\!\text{Si:} + \text{H}_2 \underset{k_{-2}}{\overset{k_2}{\rightleftharpoons}} \text{SiH}_2,$$

$$>\!\text{Si:} + \text{NH}_3 \underset{k_{-3}}{\overset{k_3}{\rightleftharpoons}} \text{Si(NH}_3)_{(ads)},$$

$$>\!\text{Si(NH}_3)_{(ads)} \underset{k_{-4}}{\overset{k_4}{\rightleftharpoons}} \text{SiNH} + \text{H}_2,$$

$$>\!\text{Si} + \text{SiH}_2 \xrightarrow{k_5} \text{SiSiH}_2,$$

$$>\!\text{SiNH} + \text{SiH}_2 \xrightarrow{k_6} \text{SiNHSiH}_2.$$

The reaction proceeding in the interior of the growing film is:

$$>\!\text{SiNH} \xrightarrow{k_7} \equiv\!\text{SiN} + \frac{1}{2}\text{H}_2.$$

In addition to the stages considered above, a side reaction of ammonia decomposition can probably proceed on the surface of the growing film:

$$2\,\text{NH}_{3(ads)} \longrightarrow \text{N}_{2(gas)} + 3\,\text{H}_{2(gas)}.$$

As the gas stream moves along the axis of the isothermal reactor, this reaction provides an increasing concentration of hydrogen in the mixture, which results in a decrease in the silicon nitride growth rate.

Taking into account the scheme of consecutive and concurrent reactions taking place on the surface of the growing film (see above), the equation for the growth rate of the dielectric film can be written in the form:

$$W = k_1[\mathbf{I}][\text{SiH}_4] + k_4[\mathbf{III}] + k_5[\mathbf{I}][\text{SiH}_2] + k_6[\mathbf{IV}][\text{SiH}_2].$$

Note that in this expression, the growth rate of structural units containing Si—N bonds is determined by the terms containing the k_4 and k_6 constants. The terms containing the k_1 and k_5 constants are responsible for the growth rate of structural units containing Si—Si bonds. This means that the stoichiometry of the films synthesised will change, depending on the reaction conditions. The rates of the stages governed by the k_5 and k_6 constants explicitly depend on the concentrations of the intermediate products of monosilane decomposition in the vapour phase (SiH_2 and SiH_3); therefore, specific features of the vapour-phase reactions will manifest themselves in the kinetics of silicon nitride film growth.

2. System $SiCl_4 - NH_3$

Experimental data on silicon nitride deposition in the $SiCl_4 - NH_3$ system have been summarised.[8, 18, 34] The silicon nitride film growth rate distribution profile along the length of the isothermal zone of a flow tube isothermal LPCVD reactor, in the temperature range 1023 – 1173 K, at $SiCl_4$ and NH_3 concentrations lying in the ranges $1\times10^{-5}-1\times10^{-4}$ and $1\times10^{-4}-2\times10^{-3}$ mol litre^{-1}, respectively, has a characteristic curve shape with a maximum, similar to the curves shown in Fig. 5. An increase in the linear flow rate of the gas mixture leads to a shift of the maximum into the interior of the reactor. These data suggest that the criterion for plug reactors is met in this case.[42] The dependence of the maximum reaction rate on the ammonia concentration at various $SiCl_4$ concentrations, and on the $SiCl_4$ concentration at a constant NH_3 concentration, show that initially the reaction rate is proportional to the NH_3 and $SiCl_4$ concentrations. At specified $SiCl_4$ concentrations, the region of zero order reaction with respect to NH_3 is clearly seen, starting from a certain concentration of $SiCl_4$. A change in the $SiCl_4$ concentration at a specified NH_3 concentration initially leads to a linear increase in the reaction rate, which is then replaced by a region corresponding to zero order with respect to $SiCl_4$. In mixtures with a large excess of ammonia, the reaction rate increases with the $SiCl_4$ concentration, faster than does a linear function.

Taking into account the characteristic dependences of the silicon nitride film growth rate on the ammonia concentration, it was assumed that the growth mechanism corresponds to a heterogeneous reaction, similar to the Langmuir – Hinshelwood reaction. This means that the process is treated as a reaction in the adsorption layer, with the reaction rate governed by the coverage of the surface of the growing film by the adsorbed $SiCl_4$ and NH_3 molecules. However, the aforementioned observations show that this assumption can only be valid for a particular set of reaction parameters. For instance, if wafers are vertically arranged in the isothermal LPCVD reactor (see Fig. 4*d*), the deposition rate depends on the spacing between wafers.[43] Analysis of the results obtained show that these features correspond to retardation at the stage of surface transformation, with allowance for diffusion supply of reagents from the vapour phase.

A strong dependence of the reaction rate on the reactor geometry was also established for the APCVD reactor at high reagent concentrations. Figure 10 presents the results obtained in two series of experiments, carried out using reactors of 67 and 14 mm diameter. As can be seen, the maximum growth rate decreases as the diameter of the reactor decreases. The results obtained can be understood if we assume that the film formation is preceded by a volume vapour-phase chemical reaction in the reactor. Therefore, the overall process must be analysed from the standpoint, according to which the synthesis of silicon nitride in the reaction of $SiCl_4$ with NH_3 proceeds as a two-path multistage reaction, controlled by the contributions of both consecutive and concurrent transformations in the vapour phase and on the surface of the growing film. Here, it is important to take into account the specific features of the chemical interactions in the $SiCl_4 - NH_3$ system.

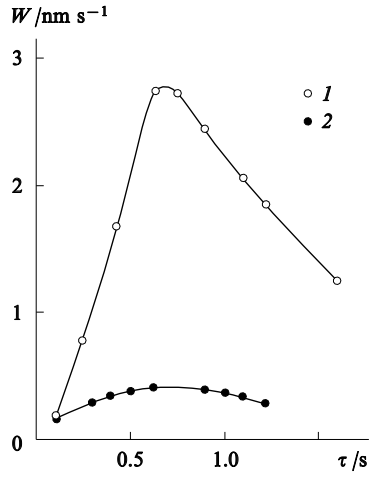


Figure 10. Silicon nitride film growth rate plotted *vs.* residence time for reactors of diameter 67 (*1*) and 14 mm (*2*).[42]
[$SiCl_4$] = 6.3×10^{-5} mol litre^{-1}, [NH_3] = 1×10^{-3} mol litre^{-1}, T = 1023 K.

Lin has shown[17] that the first intermediate product of the vapour-phase reaction is $SiNH_2Cl_3$ and that subsequent reactions result in the formation of $Si(NH_2)_2Cl$ and Si_2NHCl_6. These features can be explained assuming a multi-stage character for the reactions

$$SiCl_4 + NH_3 \rightleftharpoons Cl_3Si\cdots Cl\cdots H\cdots NH_2 \rightleftharpoons Cl_3SiNH_2 + HCl,$$

$$Cl_3SiNH_2 + HNH_2 \rightleftharpoons Cl_2(NH_2)Si\cdots Cl\cdots H\cdots NH_2 \rightleftharpoons$$

$$\rightleftharpoons Cl_2Si(NH_2)_2 + HCl, \textit{ etc.},$$

or

$$Cl_3SiNH_2 + SiCl_4 \rightleftharpoons Cl_3SiNHHCl\cdots SiCl_3 \rightleftharpoons$$

$$\rightleftharpoons Cl_3SiNH\cdot SiCl_3 + HCl.$$

The variety of polymeric particles, containing several NH_2 groups, shows that subsequent reactions proceed as a sequence of random collisions.

One can assume that the vapour-phase reaction results in $SiNH_2Cl_3$, and in the simplest case, the film growth mechanism can involve two consecutive stages with rate constants k_1 and k_2:[44]

$$SiCl_4 + NH_3 \xrightarrow{k_1} H_2N\cdot SiCl_3 \xrightarrow{k_2} Si_3N_4.$$

An expression for the maximum deposition rate in flow reactors, with inclusion of the rate constants for the reaction stages listed above, was derived for the operational regimes in the regions of zero-order reaction with respect to NH_3.[44] In its simplified form, it is as follows:

$$W_{max} \approx k_2[SiCl_4]_0\left(\frac{S}{V}\frac{k_2}{k_1}\right)^{[(V/S)(k_1/k_2)-1]^{-1}},$$

where $[SiCl_4]_0$ is the concentration of $SiCl_4$ at the beginning of the reaction zone and S/V is the surface-area-to-volume ratio of the reactor. The estimates of the rate constants are listed below:

$$k_1 = 1.3\times10^2\exp\left(-\frac{25}{RT}\right),$$

$$k_2 = 1.5\times10^{25}\exp\left(-\frac{75.3}{RT}\right)$$

(here, k_1 is given in s^{-1} and k_2 is given in molecule $cm^2\ s^{-1}$).

3. System $SiH_2Cl_2 - NH_3$

The kinetics of interactions in the $SiH_2Cl_2 - NH_3$ system in various types of reactors is much less studied, compared to other systems.[45–53] The most interesting results were obtained in the studies carried out using isothermal flow LPCVD reactors,[48–50] in which the kinetics of film growth from monosilane, dichlorosilane, dimethyldichlorosilane and silicon tetrachloride was compared directly under identical conditions.

The kinetics of silicon nitride film growth in the ammonolysis of dichlorosilane was investigated in the temperature range 1023 – 1123 K with variable reagent concentrations. The $[NH_3]/[SiH_2Cl_2]$ reagent ratio was varied from 1 to 17, the pressure varied between 60 and 1200 Pa and the linear flow rate of the gas mixture was in the range 1450 – 2870 cm s^{-1}. In this range of linear flow rates of the gas mixture along the reactor, the shape of the growth rate profiles and the absolute values of the reaction rates were constant, the deposition rate was first-order with respect to dichlorosilane and pseudo zero order with respect to ammonia at large excesses of NH_3 with respect to SiH_2Cl_2. An empirical expression for the deposition rate (in nm s^{-1}) takes the form:

$$W = 3.15\times10^{12}\exp\left(-\frac{152.3}{RT}\right)[SiH_2Cl_2].$$

Two possible mechanisms of ammonolysis of dichlorosilane have been proposed.[51–53] One of them is similar to the mechanism of the ammonolysis of $SiCl_4$, involving formation of intermediate products (*e.g.*, SiH_2NH_2Cl) and the other mechanism involves a proton abstraction and the formation of $SiCl_2$ as an intermediate. Analysis of the silicon nitride deposition rate profiles obtained for the ammonolysis of SiH_4, SiH_2Cl_2 and $SiCl_4$ (see Fig. 11 *a*) reveals

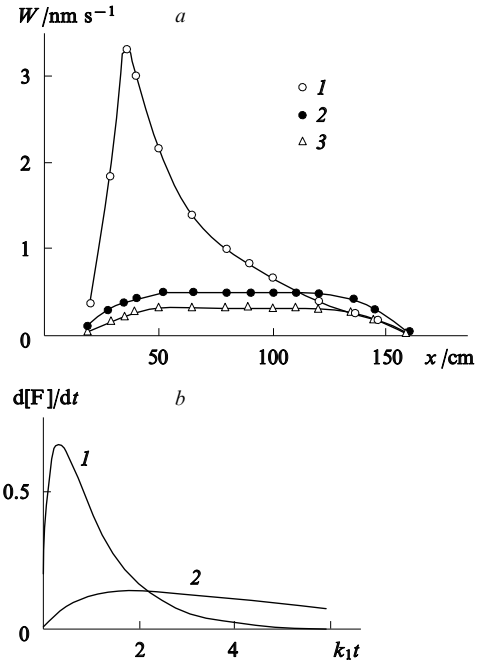


Figure 11. Silicon nitride deposition rate profiles obtained for ammonolysis of monosilane (*1*), dichlorosilane (*2*) and silicon tetrachloride (*3*) in low-pressure flow CVD reactor (*a*) and the deposition rate profiles predicted by the theory of consecutive one-side reactions for $k_2/k_1 = 5$ (*1*) and $k_2/k_1 = 0.2$ (*2*) (*b*);[49]
(*a*): concentration of silicon-containing compound is 1.86×10^{-6} mol $litre^{-1}$, 'ammonia-to-silicon-containing compound' concentration ratio is 17, $r_r = 61$ mm, $T = 1098$ K, $P = 333$ Pa, $v = 650$ cm s^{-1}.

significant differences between the mechanisms of the ammonolysis of monosilane and its chlorinated derivatives, also giving an indication of the similar mechanisms of ammonolysis of other chlorinated derivatives. Moreover, the profiles for ammonolysis of dimethyldichlorosilane, SiH_2Cl_2 and $SiCl_4$ are nearly identical, which points to the possibility of forming intermediates similar to $(CH_3)_2SiNH_2Cl$. The ammonolyses of SiH_2Cl_2 and $SiCl_4$ are characterised by similar effective rate constants in the W_{max} regions (0.74 and 0.46 cm s^{-1}, respectively) and conversions (26.6% and 18%, respectively), which are much lower than for the ammonolysis of SiH_4 (4.9 cm s^{-1} and 46.5%).

Taking into account the aforementioned observation, the growth of silicon nitride films can be correctly described in terms of a two-step reaction of homogeneous formation and heterogeneous consumption of intermediate products. The dependences of the accumulation of the end product on the reaction time (d[F]/dt) (see Fig. 11 *b*), obtained in the framework of the theory of consecutive one-side first-order reactions

$$A \longrightarrow I \longrightarrow F,$$

(A is the starting substance, I is the intermediate product and F is the end product) for the different limiting stages, are similar in shape to the curves obtained for the deposition of silicon nitride films (see Fig. 11 *a*). The limiting stage of the ammonolysis of monosilane is the formation of the intermediate product, while the ammonolysis of chlorinated monosilane derivatives is limited by the stage of heterogeneous consumption of the intermediate product.

4. Industrial methods of deposition of silicon nitride films

Since the early 1980s, the most widely used (in electronics) industrial method involves the use of dichlorosilane in flow LPCVD reactors. Typical conditions for the deposition reaction are as follows: $T \approx 973$ K at a pressure of less than 65 Pa. In this case, the deposition rates are of the order of a few hundredths of a

nanometre per second, and the thickness non-uniformity on wafers of diameters smaller than 200 mm is less than ±2% at a foreign defect (microparticles of size exceeding 0.2 μm) level of less than 0.1 defect cm^{-2}. The concentration of hydrogen in the films is ~4 at.% and the refractive index varies in the range 1.96–2.00. As old CVD equipment for electronics is replaced by single-wafer reactors (wafer diameter up to 300 mm) (see Fig. 4*b*), interest in the ammonolysis of monosilane is retained. This is due to low degree of chloride conversion and correspondingly to the extensive formation of by-products (silicoimides) that poison the vacuum systems of CVD reactors.

Low-temperature deposition of silicon nitride films from mixtures of monosilane, ammonia and/or nitrogen involves plasma activation [most often, the so-called diode systems (see Fig. 4*b*) are used][54] and occurs at temperatures below 723 K. In this case, the film composition strongly depends on the temperature and on the ammonia/monosilane ratio. Unfortunately, low-temperature silicon nitride films contain hydrogen, bonded to silicon or nitrogen; the total concentration of hydrogen exceeding 10^{21} atom cm^{-3}. Concentration depends on the deposition temperature and, for the $SiH_4-NH_3-N_2$ system, can be 20 at.%–30 at.% at 573 K and up to 5 at.%–10 at.% at 873 K. Removal of ammonia from monosilane–nitrogen mixtures on increasing in the high-frequency power supplied, allows a 25 at.%–30% reduction of the hydrogen concentration at the same deposition temperature.[55]

At lower temperatures (373–573 K) under plasma activation conditions, it is also possible to use plasma pyrolysis of organoelement compounds that simultaneously contain silicon and nitrogen (hexamethyldisilazane, hexamethylcyclotrisilazane and diethylaminotrimethylsilane). By varying the high-frequency power supplied, one can vary the concentration of CH_3 groups in the end polymeric material, which is often called 'silicon nitride'. The molecules of the starting compounds contain no Si–H bonds, which are formed during the synthesis[56] due to abstraction of protons and CH_3 groups from the molecules of the starting compounds, the formation of radicals adsorbed on the surface, followed by proton addition to broken silicon bonds. Thus, fabrication of hydrogen-free films by the plasma pyrolysis of organoelement compounds appears to be impossible.

V. Deposition of silicon oxynitride films

A number of systems were proposed for the CVD synthesis of SiON films, *e.g.*, $SiH_4-NH_3-CO_2$, SiH_4-NH_3-NO and $SiH_4-NH_3-N_2O$.[18,57] Let us consider the first system in more detail.

In deriving an expression for the deposition rate of films of various chemical compositions, one must use the mole-based units, *e.g.*, mol min^{-1} cm^{-1}. Using ellipsometric measurements of the film thickness and the refractive index, one can determine the chemical composition by a linear approximation, assuming that the refractive index, RI_{SiON}, of the silicon oxynitride film is defined through the mole fractions of silicon nitride (z_1) and silicon dioxide (z_2) (the refractive indices of silicon nitride and silicon dioxide are $RI_n = 2.025$ and $RI_{ox} = 1.45$, respectively):

$$RI_{SiON} = z_1 RI_n + z_2 RI_{ox}.$$

The growth rate, W_M (mol min^{-1}), of silicon oxynitride film can be found from the equation:

$$W_M = \frac{\rho_f S W}{M} 1.67 \times 10^{-11}.$$

Here ρ_f and M are the density and the molecular mass (they can be determined with ease using the data listed in Table 4), S is the surface area of the hot wafer and W is the growth rate (nm s^{-1}).

Experiments were carried out in a vertical non-isothermal reactor of surface area 1058 cm^2, at a gas flow rate of 1.83 dm^3 s^{-1}, under conditions where the reaction was not limited by the mass supply rate. The reaction is first order with respect to monosilane and the deposition rate is independent of the NH_3 and CO_2 concentrations in the range from 10^{-3} to 5×10^2 M. The empirical dependences of the formation of SiO_2, Si_3N_4 and silicon oxynitride SiON at 1123–1323 K are as follows:

$$k_{SiO_2} = 2.4 \times 10^5 \exp\left(-\frac{100.3}{RT}\right)[SiH_4], \quad (6)$$

$$k_{Si_3N_4} = 22.3 \times 10^5 \exp\left(-\frac{121.2}{RT}\right)[SiH_4], \quad (7)$$

$$k_{SiON} = 3.5 \times 10^5 \exp\left(-\frac{98.2}{RT}\right)[SiH_4].$$

Considering the oxynitride film growth as a reaction following two concurrent paths, *viz.*, ammonolysis of monosilane (W_n) and oxidation of monosilane (W_{ox}), the expression for W_{SiON} can be written as:

$$W_{SiON} = W_n + W_{ox}.$$

Then, assuming that the rate of formation of the structural units $SiN_{4/3}$ and $SiO_{4/2}$ is proportional to the surface coverage of the NH_3 and CO_2 molecules (Θ_{NH_3} and Θ_{CO_2}, respectively), and taking into account Eqns (6) and (7), one can write

$$W_n = k_{Si_3N_4}[SiH_4]\Theta_{NH_3}^{l_1},$$

$$W_{ox} = k_{SiO_2}[SiH_4]\Theta_{CO_2}^{l_2},$$

where l_1 and l_2 are the reaction orders with respect to their corresponding components. Assuming that NH_3 and CO_2 are the most intensely adsorbed species, we get

$$\Theta_{NH_3} = \frac{p_{NH_3}}{(\alpha_{CO_2}/\alpha_{NH_3})p_{CO_2} + p_{NH_3}},$$

$$\Theta_{CO_2} = \frac{p_{CO_2}}{(\alpha_{CO_2}/\alpha_{NH_3})p_{NH_3} + p_{CO_2}},$$

where α_{CO_2} and α_{NH_3} are respectively the constants of adsorption equilibrium between CO_2 and NH_3.

Treatment of experimental data using this approach gave the characteristic dependence of the partial rates of formation of structural units of silicon nitride and silicon dioxide, which were used to determine the coefficients l_1 and l_2 ($l_1 = 0.6$ and $l_2 = 0.5$). Generally, the rates of formation of the corresponding structural units, in the course of silicon oxynitride film growth, differ from the growth rates of the silicon nitride and silicon dioxide films. In particular, the rate of formation of $SiN_{4/3}$ in silicon oxynitride is lower than in silicon nitride, while the rate of formation of $SiO_{4/2}$ in silicon oxynitride is higher than that in silicon dioxide. However, it should also be noted that these differences are small, being only slightly larger than the scatter of experimental data.

Recently, oxynitride films used as anti-reflecting coatings in electronics have been fabricated from $SiH_4-NH_3-N_2O-N_2$ mixtures using low-temperature plasma synthesis. Such methods

Table 4. Characteristics of silicon oxynitride film.[18]

Refractive index	Molecular mass	Molar refraction	Density /g cm^{-3}
2.025	140.0	23.03	3.09
1.9	121.6	19.46	2.91
1.8	106.4	16.51	2.75
1.7	92.0	13.71	2.59
1.6	78.4	11.07	2.42
1.5	66.4	8.74	2.23
1.45	60.0	7.50	2.15

allow films of a wide range of compositions to be fabricated by varying the component ratio in the gas mixture.[54]

VI. Deposition of silicon dioxide films

Silicon dioxide films can be fabricated in the temperature range from a few hundreds of degrees to 1300 K (and higher) by oxidation, pyrolysis, hydrolysis and plasma-enhanced reactions. Below we consider the results of investigations of some most important processes in the CVD synthesis of oxide films.

1. Oxidation

Among the practically used CVD reactions, oxidation reactions are the best studied. They are conducted using monosilane, silicon, chlorides and the alkyl and alkoxy derivatives of monosilane as sources of silicon and oxygen, nitrogen oxides, CO_2, ozone–oxygen mixtures and hydrogen peroxide as oxidants. Low-temperature film deposition (at temperatures below 850 K) is performed using a plasma of the starting components.

a. System SiH_4-O_2

At present, the SiH_4-O_2 system is the best studied and most widely used in the synthesis of silicon dioxide films. This system has been the subject of long-term studies in different types of reactors as the method for synthesising of silicon dioxide films at temperatures below 720 K and as the basic system for the synthesis of complex silicate glasses.

The combustion of monosilane was first studied by Shantarovich,[58] who established a chain-radical character for this process. The 'combustion peninsula', which determines the range of the temperature and pressure values suitable for reaction in the SiH_4-O_2 system, is shown in Fig. 12. If the parameters of a system lie outside the 'combustion peninsula', the gas mixture is inert and can be kept with no apparent changes as long time as required. Thus, in any case, the reaction products (aerosil, silicon dioxide thin film or both) in the SiH_4-O_2 system are formed as a result of a branched chain process (BCP). Experimentally, the motion from the outside towards the interior of the 'combustion peninsula' (on, *e.g.*, raising the temperature with constant values for the other parameters) will give a stepwise shape to the reaction rate curve. In connection to this, attempts to explain the experimentally observed stepwise temperature dependence of silicon dioxide film deposition rate by invoking the mechanism of a reaction between the adsorbed SiH_4 and O_2 molecules on the silicon or silicon dioxide surface[59,60] (*e.g.*, the Langmuir–Hinshelwood mechanism), seem to be unsubstantiated.

The character of the monosilane oxidation reaction, which proceeds as an SiH_4-O_2 gas mixture moving along the horizontal tube reactor, is as follows: the reaction rate increases until a maximum thickness of silicon dioxide thin film is achieved,[61] and then rapidly decreases (Fig. 13 *a*,*b*). A comparison of these dependences with the temperature profile in the reactor showed that the reaction is accelerated as the temperature increases. Also of note is that the initial portions of the curves are shifted towards the inside of the reactor as the $[O_2]/[SiH_4]$ ratio increases, *i.e.*, corresponding to the points characterised by higher temperatures.

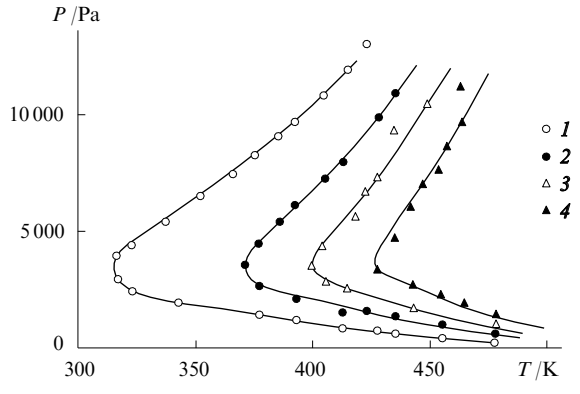


Figure 12. 'Ignition peninsula' for combustion of monosilane. $[SiH_4]$ (vol.%): 49 (*1*), 39 (*2*), 30 (*3*) and 14 (*4*).[58]

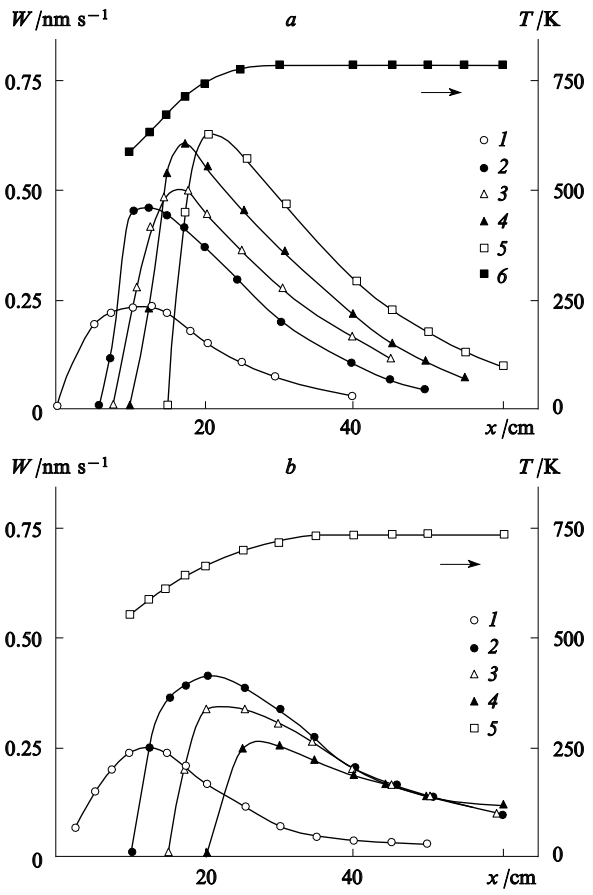


Figure 13. Silicon dioxide growth rate profiles along the reactor axis for different temperature profiles.
(*a*) $[O_2]/[SiH_4]$ = 10 (*1*), 30 (*2*), 50 (*3*), 100 (*4*), 300 (*5*); (*b*) $[O_2]/[SiH_4]$ = 10 (*1*), 70 (*2*), 120 (*3*), 180 (*4*); $[SiH_4] = 2.9 \times 10^{-2}$ mol.%, linear flow rate 19 cm s^{-1}. Curves *6* (*a*) and *5* (*b*) denote the temperature profiles in the reactor.[61]

Note that in this case, the reaction rate at the maximum of the curve is not a characteristic parameter of the process. In particular, Fig. 13 *a* shows that for the reactor with a steep temperature profile, the W_{max} value increases as the oxygen concentration in the gas mixture increases. However, in the case of a flattened temperature profile in the reactor (see Fig. 13 *b*), the maximum in the $W(x)$ dependences initially increases and then decreases as the $[O_2]/[SiH_4]$ ratio increases; as a result, we contain a dome-shaped character for the deposition rate dependences, plotted in the $W_{max}-[O_2]/[SiH_4]$ coordinates.

Using these dependences, we can compare the ignition limits of gas mixtures with the critical parameters determining the formation of silicon dioxide thin films. Data on the degree of monosilane combustion are presented in Fig. 14, and in Fig. 15 we compare the regions of SiO_2 film growth and monosilane combustion. These results show that film growth occurs only under conditions corresponding to monosilane ignition (in this case, the upper ignition limit). The film growth conditions correspond to O_2 and SiH_4 concentrations that are below the corresponding straight lines. Here, we have

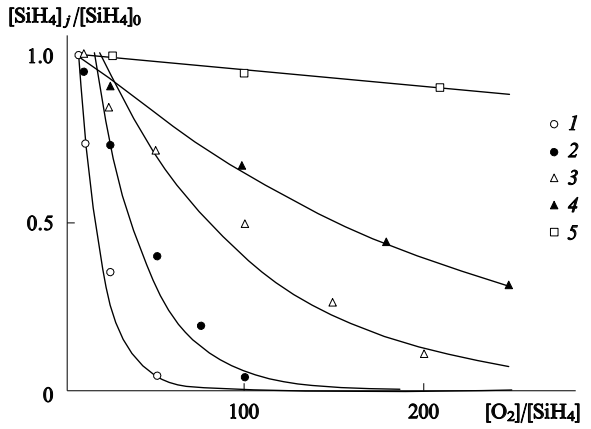


Figure 14. Degree of monosilane combustion, $[SiH_4]_j/[SiH_4]_0$, plotted *vs.* O_2 concentration.[18]
$T = 573$ (*1*), 623 (*2*), 673 (*3*), 693 (*4*), 723 K (*5*); $[SiH_4] = 8.7 \times 10^{-2}$ mol.%.

$$[O_2]/[SiH_4] = A\exp\left(\frac{-33.4}{RT}\right),$$

where A is the pre-exponent.

By studying the film growth rate distribution along the isothermal reactor zone[62,63] (Fig. 16), it is possible to establish the laws of silicon dioxide film growth under the conditions corresponding to the lower ignition limit. Particular attention should be paid to the regular increase in the growth rate towards the end of the isothermal zone. It becomes more pronounced as the partial pressure of monosilane increases and reflects the acceleration of the reaction due to the development of the branched chain process.

The limiting character of the phenomenon is illustrated in Fig. 17. We can determine the pressure (P_1), corresponding to the lower ignition limit of the gas mixture. The expression for P_1 contains the rate constants for the branching (k_b) and heterogeneous loss (k_d) of the reaction chains

$$P_1 = \frac{k_d}{2k_b f},$$

where f is the mole fraction of the component involved in the act of branching.[64]

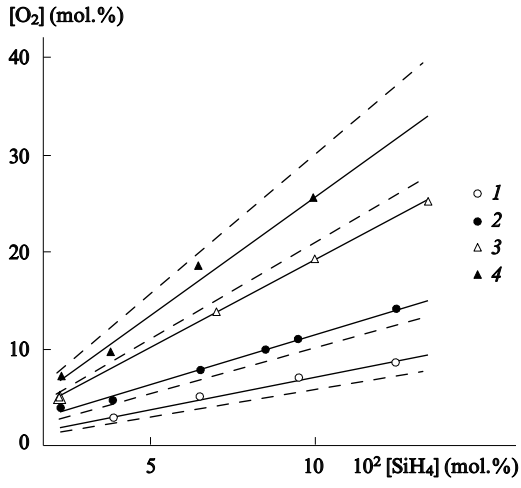


Figure 15. SiO_2 film growth regions (solid lines) and monosilane ignition regions (dashed lines).[18]
$T = 573$ (*1*), 623 (*2*), 673 (*3*), 693 K (*4*).

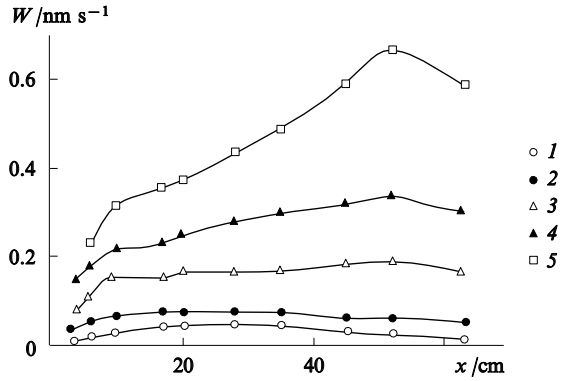


Figure 16. SiO_2 growth rate distribution in a horizontal isothermal reactor.[63]
$T = 413$ K, diameter of the reactor is 1.3 cm, the partial pressure of monosilane, Pa: 25.3 (*1*), 26.7 (*2*), 32.0 (*3*), 36.0 (*4*) and 40.0 (*5*); gas flow rate is 0.83 $cm^3\ s^{-1}$, $[O_2]/[SiH_4] = 2$.

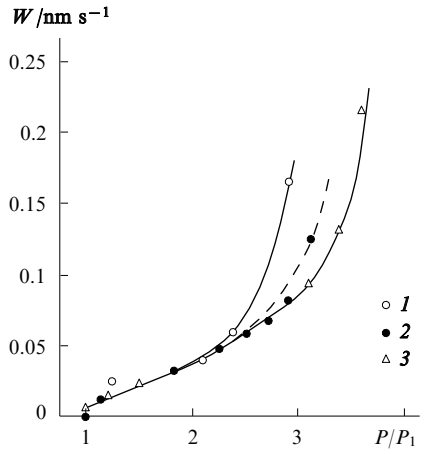


Figure 17. SiO_2 growth rate plotted *vs.* monosilane pressure in reactors of different diameters.[64]
Diameter of the reactor /cm: 2 (*1*), 1.6 (*2*) and 1.3 (*3*); $T = 373$ K; $[O_2]/[SiH_4] = 1$, gas flow rate is 0.56 $cm^3\ s^{-1}$.

In practice, the BCP studies usually involve observing the ignition of the reacting gas mixture. A number of unexpected features were disclosed in determining the lower ignition limit from the chemiluminescence of the SiH_4-O_2 mixtures.

Firstly, the position of the lower ignition limit is 'sensitive' to the state of the reactor walls. This manifests itself, in particular, in different P_1 values determined by approaching the limit using a mixture at a pressure lower than P_1 (approach from below), and by approaching the limit using higher pressures (approach from above).

Secondly, a peculiar feature of the combustion of the SiH_4+O_2 mixture is a double ignition under static conditions.[65–67] Using emission spectra, the formation of excited OH^* radicals (band at 306.4 nm) in the flame was detected.[66] An EPR study [67] revealed the presence in the flame of hydroxyl groups and oxygen atoms in concentrations of $10^{13}-10^{14}$ particle cm^{-3}. The active role of oxygen atoms in chain branching processes was proved in the experiments using inhibitors. It is known that the loss rate of oxygen atoms increases in the presence of propylene. For instance, the addition of C_3H_6 (1%) increases the lower ignition limit by 40% at 623 K.[62]

Figure 18 shows that the concentrations of oxygen atoms and hydroxyl groups increase as the $[O_2]/[SiH_4]$ ratio increases.[67] The following reactions in the flame are most probable:

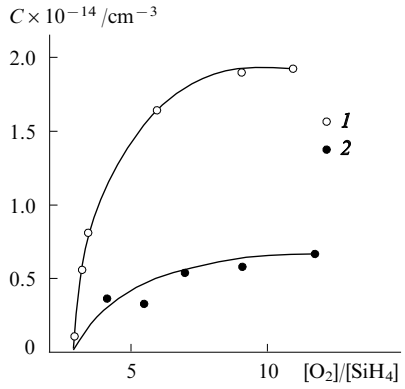


Figure 18. Concentration of oxygen atoms (*1*) and hydroxyl groups (*2*) plotted *vs.* $[O_2]/[SiH_4]$ ratio in the initial mixture in SiH_4 flame.[67] Total pressure is 400 Pa, $T = 723$ K.

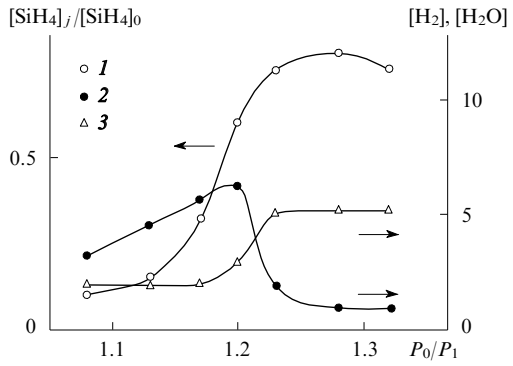


Figure 19. Degree of silane combustion $[SiH_4]_j/[SiH_4]_0$ (*1*) and yields of the end gaseous products H_2 (*2*) and H_2O (*3*) (rel. u.) plotted *vs.* the P_0/P_1 ratio for a 9.4% SiH_4 + 64% O_2 + 26.6% He mixture at 423 K and $P_1 = 203.9$ Pa.[73]

$$O + SiH_4 \longrightarrow {}^{\bullet}SiH_3 + OH,$$

$$OH + SiH_4 \longrightarrow {}^{\bullet}SiH_3 + H_2O.$$

Radicals $^{\bullet}SiH_3$, present in the vapour phase, were detected by laser magnetic resonance. The concentration of $^{\bullet}SiH_3$ radicals in the monosilane flame[68] was 4×10^{13} particle cm^{-3}. Analysis of the luminescence spectrum showed that the $^{\bullet}OH$ radicals are in an electronic excited state and the energy of the emission quantum is 388 kJ mol^{-1}. This suggests the occurrence of the following reaction

$$O + H + L \longrightarrow {}^{\bullet}OH + L,$$

where L is the molecule involved in ternary collision. Indirect measurements showed that $[O][H] \approx 10^{26}$ particle^2 cm^{-6} s^{-2}. In addition to the particles mentioned above, electronically excited SiO* molecules (band $A'\Pi - X'\Sigma +$, emission quantum energy 504 kJ mol^{-1}) were identified using the luminescence spectra. No more reliable data on the composition of the gas phase in the monosilane flame are available at the moment. At the same time it must be remembered that Shantarovich [58] assumed the presence of an intermediate, silanone H_2SiO ('silicon aldehyde'). Products containing silicon–oxygen double bonds [silanone H_2SiO, silanoic acid HSiOH and silicic acid $(HO)_2SiO$] were detected only in an argon matrix at 17 K.[69]

When analysing the data on the kinetics of monosilane oxidation, the possibility of the formation of short-lived products must be taken into account. The inclusion of their properties allows one to establish the mechanism of the formation of finely dispersed aerosil (SiO_2) powder, which usually accompanies the growth of SiO_2 films.

Calculations [70] of the following dimerisation reaction

$$2\,H_2SiO \longrightarrow (H_2SiO)_2$$

showed that the formation of the four-membered ring occurs barrierlessly and that the enthalpy of reaction is $\Delta H^{\circ}_{298} = -441.8$ kJ mol^{-1}. The formation of trimers and tetramers is also characterised by a large exothermic effect. Silanone decomposition by the reaction

$$H_2SiO \longrightarrow H_2 + SiO$$

was shown [71] to be hampered because its activation energy is 358.6 kJ mol^{-1}. Dimerisation of SiO proceeds barrierlessly.[72] Two more end products, H_2 and H_2O, were identified in the vapour phase. In relation to this, two possible routes of monosilane combustion are discussed:

$$SiH_4 + O_2 \longrightarrow SiO_2 + 2\,H_2,$$

$$SiH_4 + 2\,O_2 \longrightarrow SiO_2 + 2\,H_2O.$$

Quite reliable data are available, showing that the formation of water in the vapour phase is not due to subsequent combustion of hydrogen.[73] Analysis of the dependence (see Fig. 19) of the degree of monosilane combustion on the P_0/P_1 ratio (P_0 is the initial pressure in the mixture) shows that the hydrogen/water concentration ratio also varies with the P_0/P_1 parameter. Water molecules can be formed as a result of the vapour-phase reaction and as a product of desorption from the surface of solid SiO_2 particles. For this reason, no exact reaction equation for monosilane combustion has been derived to date.

Atoms and radicals produced in the combustion of monosilane in oxygen in the vapour phase are highly reactive species; their recombination on the surface results in the formation of silicon dioxide structural units. Some types of interactions can be established using the bond dissociation energy values. For instance, the reaction

$$SiH_4 + O \longrightarrow H_2SiO_{2/2} + H_2$$

produces a surface silicon atom bonded to two hydrogen atoms and to the oxide matrix through two bridging oxygen atoms. The reaction requires an energy expenditure for the breaking of two Si–H bonds; the formation of products will be accompanied by the release of the energy of two Si–O bonds and the energy of formation of the H_2 molecule. This approach was used for the evaluation of thermal effects for different types of structural units (Table 5).

In analysing these data, considerable attention must be paid to the high thermal effect of forming the main structural unit, the

Table 5. Enthalpies of formation of structural units in the Si–H–O system.[18]

Structural unit	Reaction	$-\Delta H$ /kJ mol^{-1}
$SiO_{4/2}$	$SiH_4 + O_2 \longrightarrow SiO_{4/2} + 2\,H_2$	802
$H_2SiO_{2/2}$	$SiH_4 + O_2 \longrightarrow H_2SiO_{2/2} + H_2O$	643
$SiO_{4/2}$	$(HO)_2SiO_{2/2} \longrightarrow SiO_{4/2} + H_2$	522
$SiO_{4/2}$	$HSiO_{3/2} + OH \longrightarrow SiO_{4/2} + H_2$	539
$H_2SiO_{2/2}$	$SiH_4 + O_2 \longrightarrow H_2SiO_{2/2} + H_2$	643
$H_2SiO_{2/2}$	$SiH_4 + O \longrightarrow H_2SiO_{2/2} + H_2$	647
$HSiO_{3/2}$	$H_2SiO_{2/2} + OH \longrightarrow HSiO_{3/2} + H_2$	539
$(HO)HSiO_{2/2}$	$H_2SiO_{2/2} + O \longrightarrow (HO)HSiO_{2/2}$	62
$(HO)_2SiO_{2/2}$	$(HO)HSiO_{2/2} + O \longrightarrow (HO)_2SiO_{2/2}$	62
$SiO_{4/2}$	$H_2SiO_{2/2} + O \longrightarrow SiO_{4/2} + H_2$	647
$H_2SiO_{2/2}$	$SiH_3 + O \longrightarrow H_2SiO_{2/2} + H$	581
$H_2SiO_{2/2}$	$SiH_2 + O \longrightarrow H_2SiO_{2/2}$	852
$SiO_{4/2}$	$SiH_3 + O_2 \longrightarrow SiO_{4/2} + H + H_2$	702
$SiO_{4/2}$	$SiH_2 + O_2 \longrightarrow SiO_{4/2} + H_2$	974

$SiO_{4/2}$ tetrahedron, and the structural unit $H_2SiO_{2/2}$, a building block with a two-dimensional chain structure. Account must also be taken of the fact that breaking of single chemical bonds with oxygen atoms is, as a rule, characterised by low activation energies [74] (usually, at most 16.7 kJ mol^{-1}). This suggests that the main direction of reactions is determined by the stages involving oxygen atoms rather than molecules.

The most practically valuable problems in the synthesis of silicon dioxide thin films by the oxidation of monosilane with oxygen are the formation of aerosil, non-stationarity in the deposition process and the porosity of silicon dioxide films.

The essence of the first problem is that the sizes of aerosil microparticles are comparable with or larger than the size of elements of microelectronic devices. Therefore, it is highly probable that a microparticle arriving at the wafer surface during the film synthesis will be a reason for improper operation of the device. In relation to this, the level of microdefects in thin films is one of the most important characteristics of industrial CVD reactors. For instance, at the end of the twentieth century in semiconductor electronics, the level of extra film defects for CVD processes was less than 0.1 defect cm^{-2} for the wafer surface at microparticle sizes exceeding 0.2 μm. Using microprobe analysis on the vapour phase in the film synthesis zone, it was established that aerosil microparticles are formed in the oxidation of monosilane by oxygen in all types of reactors.[75–77]

Various studies [63, 78–82] are of interest from the standpoint of determining the conditions for the growth of defect layers. They were carried out at relatively low deposition temperatures (373–673 K) and reagent pressures (< 133 Pa) in reactors of different sizes. A qualitative picture of the arrangement of the silicon dioxide film growth and aerosil formation regions, at constant values of other parameters, is shown in Fig. 20. The *AB* line in Fig. 20*a* corresponds to the limiting pressure P_1 (no reaction occurs below P_1). At $P > P_1$, silicon dioxide films are formed in the region above the portion of the *AB* curve (solid line) and below the pressure limiting line (dashed line). Above the dashed line lies the region of aerosil formation. As the temperature decreases, the range of pressures ($\Delta P = P - P_1$) suitable for the fabrication of dioxide films regularly narrows. Below a certain temperature at $P > P_1$ (where the curve of the limiting pressure is shown as a dashed line) the exclusive reaction product is aerosil.

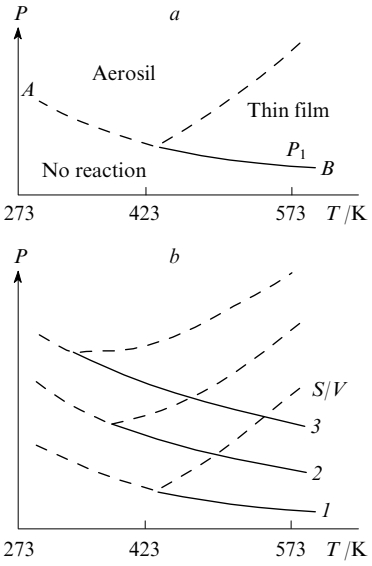


Figure 20. Regions of SiO_2 thin-film growth and aerosil formation in the SiH_4-O_2 SiO_2 system (*a*) and influence of the reactor surface-to-volume ratio on positions of these regions, $(S/V)_1 < (S/V)_2 < (S/V)_3$ (*b*). For details, see text.[78]

Analysis of the dependences shown in Fig. 20*b* reveals a general trend, namely, the growth regions are shifted as the ratio of the inner surface area, *S*, to the volume, *V*, of the reactor, in the deposition zone, changes. As can be seen, the S/V parameter increases as the number of the curve increases. The effect of the S/V ratio on the film growth conditions in reactors of different sizes has been studied in detail.[63] The deposition was performed in quartz tube reactors with horizontally arranged wafers. It was found that at a specified temperature, pressure and $[O_2]/[SiH_4]$ ratio, the P_1 values are inversely proportional to the diameter of the reactor (*i.e.*, they increase with an increase in the S/V ratio, which is characteristic of the BCP). It is important to note that an increase in the S/V ratio (decrease in the diameter of the reactor) is accompanied by (i) an increase in the limiting pressure P_1 and (ii) a simultaneous regular shift of the region of formation of silicon dioxide thin films towards low temperatures; moreover, the aerosil formation boundary is also shifted. This is an indication of improved conditions for the synthesis of defect-free thin films.

Thus, only by varying the reactor geometry, is it possible to carry out the reaction in any of the three regions shown in Fig. 20*a*. By varying the S/V ratio within certain limits in the film growth region, one can also change the film growth rate (this parameter will decrease with an increase in the S/V ratio). In practical implementations of the BCP for the fabrication of defect-free silicon dioxide thin films, the S/V ratio must be increased by exclusion of the 'extra volumes' in reactors by, *e.g.*, filling the gaps on both sides of wafers in the tube reactor (see Fig. 4*d*) with hollow vessels of the same external diameter as the wafers in order to retain the gas-dynamic parameters of the reactor.

The second and third problems are characteristic of very low-temperature (373–473 K) conditions for film deposition in the SiH_4-O_2 system. When SiO_2 is deposited at such temperatures, the kinetics of film growth is strongly dependent on the state of the inner surface of the reactor.[78, 79] The state of the surface (first of all, the composition and structure) governs its adsorption capacity and chain loss efficiency. Changes in these properties cause changes in the rates of the heterogeneous stages, branched chain reactions and SiO_2 film deposition at constant pressure, temperature and concentration of starting reagents. Even if the parameters of the deposition process can be preset and maintained at constant levels, the chemical state of the reactor surface still cannot be controlled, but it is this factor that affects the kinetics of the chain process and leads to non-stationarity of the growth rate in the initial stages. This kind of non-stationarity will be observed until the coverage of the whole reactor surface with a new SiO_2 film is complete. When the surface of the growing film is covered by the adsorption layer of a specified composition, which is reproduced in the course of further deposition, the growth rate takes a constant value. If deposition begins in a reactor whose surface was preliminarily covered with a silicon dioxide film (so-called 'modified reactor'), theoretically no transient processes would occur. This is not the case however, because the chemical properties of the surface are determined by the composition of the reacting gas mixture, from which the material is formed. Therefore, the surface properties of the newly formed silicon dioxide film will, as a rule, be different from those of the starting oxide, *i.e.*, the transient process will also occur in the modified reactor.

The kinetics of the initial stages of silicon dioxide film growth, until a thickness of 10–20 nm, was studied *in situ* using a fast automated ellipsometer.[79] The results obtained were summarised in the form of a diagram plotted in 'pressure of the starting gas mixture (P)–chain loss efficiency' (β) coordinates and shown in Fig. 21. The β value characterises the change in the chemical state of the surface in the course of deposition. The *ab* curve drawn conditionally (the particular shape of this dependence cannot be obtained from experimental data, but it is known that P_1 increases with increasing β) shows the change in the limiting pressure P_1 upon an increase in β. Below this curve lies the region corresponding to no reaction. The shaded region meets the quasi-stationary growth conditions. Experiments showed that the process always

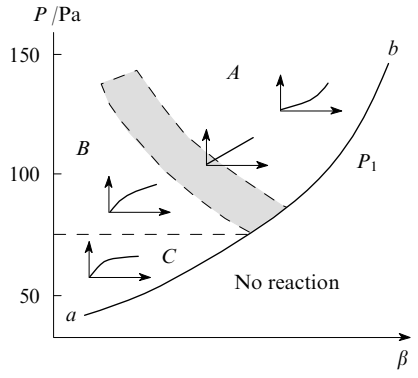


Figure 21. Regions with different kinetics of the initial stages of SiO_2 thin film growth.[78]
For details, see text. P_1 is the limiting pressure.

develops towards quasi-stationary growth. Depending on which direction we move along the curve (to the right or to the left), the β and, correspondingly, P_1 values can decrease or increase.

The shape of the kinetic curves is governed by the initial conditions, *viz*., the pressure and the chemical state of the surface. In the regions *A*, *B* and *C* (see Fig. 21) we schematically show the kinetic curves which are observed in the initial stages of growth, plotted in the 'film thickness – film growth time' coordinates. Film growth in region *A* occurs with acceleration and in the regions *B* and *C* with retardation. No stationary film growth occurs in region *B* because the growth rate decreases down to zero. Thus, all the experimentally observed shapes of the kinetic curves, which characterise the non-stationarity of the process in its initial stages, are explained by a concept of a transient process of new surface formation on the reactor walls and wafer. The properties of this surface are determined by the deposition conditions.

In studies of the kinetics of film growth until the thickness 100 – 1000 nm, using a quartz crystal microbalance, it was found that at temperatures below 523 K, the quasi-stationary growth, which follows the dramatic change in the growth rate in the initial stages, is retained until a thickness of 20 to 30 nm. Further increase in the film thickness leads to a monotonic (much slower compared to the changes in the initial stage) decrease in the growth rate.[78] The lower the synthesis temperature and the higher the pressure of the gas mixture, the more pronounced the decrease in the growth rate; in long-term experiments, the growth rate can decrease to zero.

In these experiments, the deposition rate decreases after completion of the initial transient period, in wich a SiO_2 layer is grown in the reactor. This means that retardation of the BCP in the course of film growth is due to other reasons, not associated with the change in the chemical state of the surface. A qualitative explanation for the decrease in the growth rate observed in this thickness range is as follows. Growth of a film is accompanied by the formation of its macro- and microstructure, which are to a great extent determined by the deposition conditions. An adsorption porosimetry study[80] showed that a large number of mesopores of diameter 3 to 10 nm, connected to the surface, were formed in the film under the experimental conditions. The appearance of open pores increases the real surface area of the growing film and the permeability of the film to the diffusion of the sorbed particles towards the near-surface region of the film. Taken altogether, this favours the extension of the heterogeneous reaction zone, leads to more efficient chain loss per unit surface area and, correspondingly, to a decrease in the BCP rate.

This explanation is substantiated by the following experimental results. It was found[80] that the porosity of thin films synthesised at temperatures below 523 K dramatically decreases upon introduction of small amounts of ammonia into the monosilane – oxygen gas mixture. Deposition of these films must not cause a marked increase in the real surface area. If the deposition rate decreases due to the formation of the porous structure, the growth rate of such films must be independent of time. Indeed, a qualitative difference between the kinetics of thin film growth in the presence and in the absence of ammonia additives was found.[81] In the presence of ammonia the growth rate was independent of time until a thickness of at least 1000 nm was achieved. A constant growth rate of thin films was also observed at temperatures above 523 K because the porosity of the deposited thin film dramatically decreases with increasing synthesis temperature.

Non-stationarity of the growth of silicon dioxide thin films at low temperatures (below 573 K) and low pressures can be explained by the superposition of two processes with different dynamics, a fast process of maximum duration 120 s and a slow one. The fast process is due to the change in chemical state of the surface in the course of deposition. The slow rate decrease process is associated with changes in the real film surface owing to the formation of mesopores connected to the surface in the course of deposition. In addition to the effect of temperature on the porosity of silicon dioxide films, it is also affected by the total pressure in the course of deposition. This fact is illustrated by the dependence of the minimum pore size on the total pressure, obtained at temperatures below 473 K (Fig. 22).

The problem of aerosil formation (see above) gave an impetus to search for methods of control (in fact, inhibition) of the BCP, including the problem of improving the conformality of film deposition on stepwise reliefs. As a possible variant, the effect of such inhibitors as C_2H_4, C_2H_6, C_2H_2, NH_3, NO and NO_2 on the oxidation of monosilane by oxygen was studied.[83,84] As can be seen from Fig. 23, C_2H_2 and NO have no effect on the reaction,

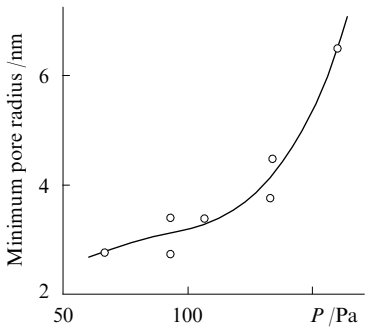


Figure 22. Minimum pore radius plotted *vs*. total pressure during the formation of SiO_2 layer in the $SiH_4 - O_2$ system.[82]

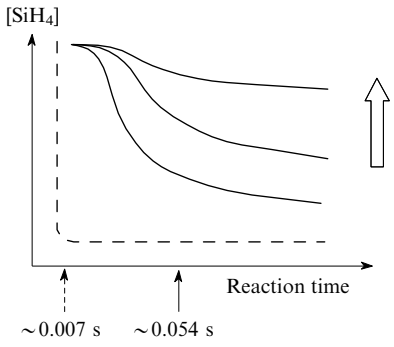


Figure 23. Illustration of the effect of the increase in the concentration of inhibitors (large vertical arrow) in the $SiH_4 - O_2$ gas mixture on the rate of monosilane consumption.
Dashed line and dashed arrow denote the dynamics and the time of complete consumption of monosilane under inhibitor-free conditions, solid arrow denotes the time corresponding to wafer position in the reactor.[83]

while other compounds inhibit the oxidation of monosilane. In this case the situation on a wafer, whose arrangement in the reactor was characterised by a particular reaction time, is as follows. The silicon dioxide film growth rate correspondingly decreases and the conformality of deposition on the lateral surfaces of gaps in complex-shape reliefs is significantly improved. Nevertheless, it is now impossible to fundamentally improve the quality of deposited silicon dioxide films by the known methods of control of the BCP of monosilane oxidation by oxygen. Consequently, other chemical systems have been the subject of intensive research since the late 1970s.

b. System $SiH_4 - N_2O$

In the $SiH_4 - N_2O$ system, SiO_2 can be fabricated at temperatures above 773 K (higher than in the case of the $SiH_4 - O_2$ system). By varying the $[N_2O]/[SiH_4]$ ratio it is possible to vary the film composition continuously from amorphous/polycrystalline silicon at $[N_2O] = 0$ to oxygen-doped polycrystalline silicon of composition SiO_y ($y < 2$) at $0.2 < [N_2O]/[SiH_4] < 10$ and further for silicon dioxide at $[N_2O]/[SiH_4] > 50$. Strictly speaking, in the first two cases, we are concerned with semiconductor or semi-insulating films rather than dielectric ones; therefore, they are of specific interest.‡

In flow LPCVD reactors amorphous silicon films are fabricated at a deposition temperature of ~ 823 K, and polycrystalline silicon films at temperatures above 893 K. The growth rate of polycrystalline silicon films depends on the reaction development time (it rapidly decreases starting at 0.05 s). In the initial stages, the deposition rate of polycrystalline silicon films depends strongly on the wafer material. Until a film thickness of ~ 22 nm, the deposition rates are relatively low and therefore we can talk of an induction period in the film growth. This period is determined by the duration of the growth stages of individual nuclei, their outgrowth and their closure into a continuous layer. After completion of the induction period, the growth continues on the surface of polycrystalline silicon film, the growth rate being independent of the characteristics of the wafer material. In a particular range of pressures, the deposition rate is governed by first-order processes with respect to SiH_4. The temperature dependence of the growth rate is characterised by an activation energy of 148.8 kJ mol^{-1} for low degrees of monosilane conversion and of 218.2 kJ mol^{-1} for high conversions. The activation energy at low conversions depends on the wafer material. Pyrolysis of SiH_4 follows two concurrent paths and results in the formation of reactive silylene (SiH_2) molecules and silyl radicals $^{\bullet}SiH_3$. The intermediate products involved are Si_2H_6 and Si_3H_8. The presence of SiH_2 and $^{\bullet}SiH_3$ in the vapour phase will lead to a more intense adsorption of these species on the growing surface, while the presence of polysilane molecules in the vapour phase favours the formation of silicon clusters in the vapour phase.

At a preset SiH_4 concentration, the overall growth rate of oxygen-doped polycrystalline silicon (SiO_y) films changes in a complex manner[86] (Fig. 24 *a*). As can be seen, until $[N_2O]/[SiH_4] = 10$ the growth rate decreases as follows

$$W = \frac{W_{Si}}{1 + g_{N_2O} p_{N_2O}},$$

where W_{Si} is the growth rate of the polycrystalline silicon film, g_{N_2O} is a constant and p_{N_2O} is the partial pressure of N_2O. At $[N_2O]/[SiH_4] > 10$, the growth rate monotonically increases, and at $0.05 < [N_2O]/[SiH_4] < 0.6$, the y value changes almost linearly between 0 and 1.25 (Fig. 24 *b*).[87,88] The film growth rate distribution along the length of the reactor at reaction times no longer than 0.01 s exhibits a characteristic rate maximum; this feature

‡ The readers who are interested in this problem are directed to Refs 18 and 85–88, which present a comprehensive treatment of the growth kinetics of such films.

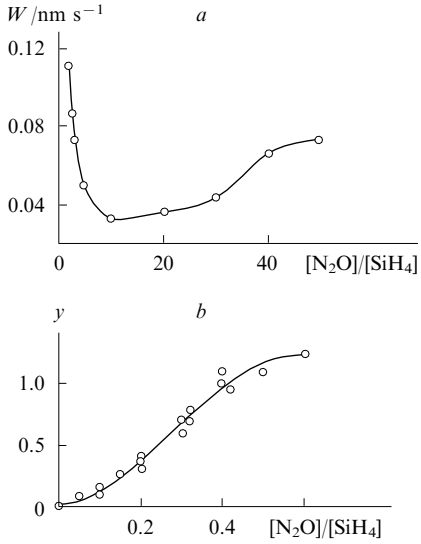


Figure 24. Growth rate (*a*) and oxygen content (*b*) in silicon-doped SiO_2 thin films plotted *vs.* $[N_2O]/[SiH_4]$ ratio.[86]
(*a*): $T = 913$ K, $[SiH_4] = 8.0 \times 10^{-7}$ mol litre^{-1}; (*b*): $T = 923$ K.

permits a quantitative description of the process. The temperature dependence of the deposition rate is characterised by an activation energy of 140.8 ± 4.0 kJ mol^{-1}.

The growth of oxygen-doped polycrystalline silicon films is governed by the laws of the reactions taking place in the adsorption layer. In connection with this mention may be made that a direct experimental proof of the adsorption of N_2O molecules on the silicon dioxide surface was obtained. It is noteworthy that the constants of the adsorption equilibria on the SiO_2 surface for SiH_4 and N_2O (g_{N_2O} and g_{SiH_4}, respectively) are comparable.[86] The dependence shown in Fig. 24 *a* can be treated as follows: the film growth rate decreases as the pressure of N_2O increases due to the competitive adsorption of SiH_4 and N_2O onto the same active sites.

The growth of SiO_2 films in the system under study occurs at $[N_2O]/[SiH_4] > 50$.[89–91] The process can conveniently be observed in the temperature range 833–1073 K. The deposition rate profiles along the reactor axis are presented in Fig. 25. Maxima in the deposition rate profiles correspond to the inner part of the reactor; the higher the monosilane concentration in the mixture, the larger the shift of the maximum. The initial portions of the

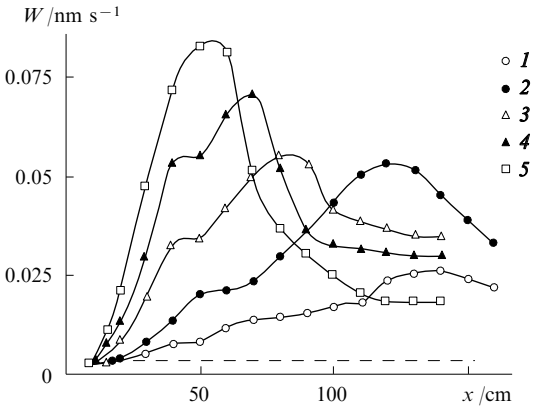


Figure 25. Growth rate distribution of SiO_2 thin films in an atmospheric pressure isothermal reactor.[90]
The partial pressure of SiH_4 is 10.6 Pa; the partial pressure of N_2O /kPa: 2.0 (*1*), 5.1 (*2*), 8.1 (*3*), 15.2 (*4*) and 30.7 (*5*). Dashed line denotes the isothermal zone for $T = 833$ K.

curves are linear, their slopes being proportional to the pressure of N_2O. In the temperature range 1023–1073 K the growth rate maxima correspond to the beginning of the isothermal zone; in the inner part of the reactor the growth rates dramatically decrease. From these plots it follows that below 973 K, the rate of the process is described by the expression

$$W = k_1 p_{N_2O_{(0)}} + k_2 (p_{N_2O_{(0)}} - p_{N_2O_{(x)}}),$$

where k_1 and k_2 are the rate constants and $p_{N_2O_{(0)}}$ and $p_{rmN_2O_{(x)}}$ are the partial pressures of N_2O at the beginning of the isothermal zone and at a point x on the axis of the reactor, respectively.

This equation reflects the fact that the reaction follows two paths. One of them, with the rate constant k_1, is responsible for the adsorption mechanism of SiO_2 formation. The other path, characterised by the rate constant k_2, determines the effect of the vapour-phase reactions on the growth of SiO_2 films. Involvement of the vapour-phase stages of the reaction is directly observed upon introduction of small concentrations of radical inhibitors into the vapour phase. For instance, the addition of less than 1% of ethylene or propylene into the gas mixture causes the growth rate at 873 K to decrease several-fold. The same additives introduced at 1073 K cause only a 20%–25% decrease in the growth rate. The temperature dependence of k_1 is characterised by an activation energy of 196 kJ mol^{-1}, the pre-exponent being equal to 1.7×10^{11} Å min^{-1} (mm Hg)$^{-1}$.

Thus, the two-path process of SiO_2 film growth involves two concurrent reactions. These are the heterogeneous reaction between adsorbed SiH_4 and N_2O molecules and the vapour-phase autocatalytic or chain reaction, involving the products of N_2O decomposition. Most probably, the chain reaction of monosilane oxidation with oxygen, produced in the heterogeneous decomposition of N_2O, accelerates the overall reaction.

The empirical relationships for evaluating the deposition rates (at $T = 923$ and 1023 K) in isothermal reactors with a dense cross-vertical arrangement of wafers (with ~15 mm spacings) (the deposition rate of SiO_2 is given in nm s^{-1}) are as follows:[91]

$$W_{923} = 1.67 \times 10^{-5} p_{SiH_4}^{0.5} p_{N_2O},$$

$$W_{1023} = 5.0 \times 10^{-7} \left(320 - \frac{p_{N_2O}}{p_{SiH_4}}\right) p_{SiH_4}^{0.5} p_{N_2O}.$$

The assumption of a branched chain component of the oxidation of monosilane by N_2O (this unambiguously indicates the possibility of formation of the aerosol phase under CVD conditions) was experimentally proved by studies of the conditions for intense nucleation in the vapour phase, using gas mixtures of preset composition.[91] The film surfaces were checked for the presence of microparticles using an optical microscope and by scattering with photons produced by a He-Ne laser (laser light was introduced through transparent windows parallel to the axis of a flow isothermal hot-wall reactor); the light intensity was measured using a photodiode. For a known composition of gas mixture, light scattering began after a specific total pressure in the reactor had been exceeded. Once determined, the pressure values for the mixture compositions under study can be used to calculate the corresponding critical partial pressures of N_2O and SiH_4.

A generalised diagram, presented in Fig. 26, shows the regions of formation of reaction products in the form of thin films and aerosol for the deposition temperature 923 K. A correlation between the defects in the deposited film and the growth rate is apparent. Namely, defect-free silicon dioxide films grow in region *I* at rather low rates; region *II* corresponds to the appearance of microparticles on the surface of the silicon dioxide film, growing at a higher rate (the microparticles can be seen in the optical microscope); region *III* corresponds to intense nucleation in the vapour phase, where both the reactor walls and wafers become covered with a powder. The limiting growth rates of 'defect-free' silicon dioxide films in region *I* at the deposition temperatures 923, 1023 and 1123 K were estimated at ~0.08, ~0.17 and ~0.12 nm s^{-1}, respectively.

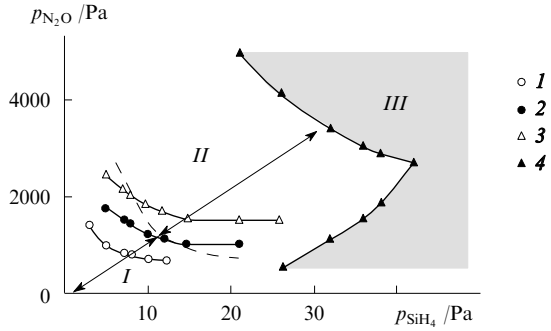


Figure 26. Regions of formation of the products of oxidation reaction: defect-free thin film (*I*), defect thin film (*II*) and aerosol (*III*) for the CVD process in the SiH_4-N_2O system at 923 K.[91]
Growth rate /nm s^{-1}: 0.033 (*1*), 0.066 (*2*) and 0.099 (*3*). Dashed line denotes the boundary between the regions *I* and *II* and curve *4* is the boundary of the region of aerosol formation (shaded).

c. Systems SiH_4-NO and SiH_4-NO_2

Depending on the concentration ratio of SiH_4 and NO in the SiH_4-NO system, both silicon dioxide (at $[SiH_4]/[NO] < 0.25$) and silicon oxynitride (at $[SiH_4]/[NO] = 0.5-1.0$) films can be fabricated. The reaction

$$SiH_4 + 4\,NO \longrightarrow SiO_2 + 2\,H_2O + 2\,N_2$$

was studied at low degrees of conversion.[92]

The activation energy for this process is 125.4 kJ mol^{-1}. Studies on the character of the adsorption processes on the surface of silicon at room temperature and an exposure of 10 Langmuir revealed[93,94] dissociative adsorption of NO and a monolayer coverage of the surface with the same coverages, equal to 0.5, for both oxygen and nitrogen atoms.

At a temperature of ~723 K and a pressure of ~133 Pa, the reaction proceeds slowly and obeys the laws of heterogeneous kinetics. As the pressure increases, the reaction is dramatically accelerated and intense chemiluminescence in the vapour phase is observed.[92]

d. System SiH_4-CO_2

The deposition of silicon dioxide films in the SiH_4-CO_2 system was studied in the temperature range 973–1373 K at $[CO_2]/[SiH_4] = 100$.[95,96] The deposition rate increases as the concentrations of both components increase, being higher in argon than in hydrogen. The two possible reaction routes are as follows:

$$SiH_4 + 4\,CO_2 \longrightarrow SiO_2 + 4\,CO + 2\,H_2O,$$

$$SiH_4 + 2\,H_2O \longrightarrow SiO_2 + 4\,H_2.$$

The presence of excess silicon in the SiO_2 films also indicates the occurrence of a concurrent reaction, *viz*., the thermal decomposition of monosilane.

e. System $SiH_4-H_2O_2$

The $SiH_4-H_2O_2$ system, at a deposition temperature similar to room temperature and a reduced pressure, was proposed in order to solve a topical problem of the high-quality filling of gaps between elements with complex reliefs in microelectronic devices.[97] The kinetics of film growth have not been reported as yet, but it was established that the main factor affecting the deposition rate is pressure. It is assumed that the oxidation reaction

$$SiH_4 + 2\,H_2O_2 \longrightarrow Si(OH)_4 + 2\,H_2,$$

is followed by polymerisation and the formation of a silicon dioxide film:

$$n\,Si(OH)_4 \longrightarrow H[OSi(OH)_2]_nOH + (n-1)\,H_2O \longrightarrow$$
$$\longrightarrow n\,SiO_2 + (n+1)\,H_2O.$$

f. Oxidation of chlorinated and organic derivatives of monosilane

The $SiH_2Cl_2-N_2O$, $(CH_3)_2SiCl_2-N_2O$, $SiH_2Cl_2-O_2$ and $(CH_3)_2SiCl_2-O_2$ systems were studied in LPCVD reactors at temperatures 1023–1123 K.[30, 45, 46, 98] However, almost no kinetic data were reported. The first three systems are characterised by very low deposition rates (at most 0.016 nm s^{-1}) and a high sensitivity of the deposition processes on the total pressure in the reactor; a feature of the $SiH_2Cl_2-O_2$ system is an intense aerosil formation. In all of these systems, the film thickness uniformity across the wafer is very low, but only the $SiH_2Cl_2-N_2O$ system is used in high-precision technologies. The reaction for this system has the form:

$$SiH_2Cl_2 + 2\,N_2O \longrightarrow SiO_2 + 2\,N_2 + 2\,HCl.$$

The $(CH_3)_2SiCl_2-O_2$ system appeared to be the most promising for the fabrication of silicate glass films at admissibly high temperatures, because the deposition rates under identical conditions were nearly an order of magnitude higher.[30, 98] The experiments were carried out using isothermal LPCVD reactors (see Fig. 4 *c*,*d*) at pressures 260–775 Pa in the temperature range 1023–1123 K. The deposition rate profiles in the reactors exhibited portions characterised by low deposition rate constants (a plateau), after which the growth rates increased. The plateau region became smaller as the pressure and temperature increased. The reaction is nearly first-order with respect to $(CH_3)_2SiCl_2$, while with respect to O_2, the reaction changes from a first-order process to a higher-order one.

$SiCl_4$ and O_2 interact at temperatures > 1430 K [99, 100] following the reaction:

$$SiCl_4 + O_2 \longrightarrow SiO_2 + 2\,Cl_2.$$

Reactions at temperatures 1073–1173 K result in thin films of two oxychlorides, Si_2OCl_6 and cyclic oxychloride, $Si_4O_4Cl_8$. The oxidation of tin and titanium tetrahalides by oxygen at temperatures below 1073 K were also studied in order to obtain tin and titanium oxide films, respectively.[18]

g. Systems $C_2H_3Cl_2CH_3SiH_2-O_2$ and $(CH_3CO_2)_2(C_4H_9O)_2Si-O_2$

Reactions in the $C_2H_3Cl_2CH_3SiH_2-O_2$ and $(CH_3CO_2)_2.(C_4H_9O)_2Si-O_2$ systems were assumed to be alternatives to the BCP in the low-temperature oxidation of monosilane, but they have found no practical applications because of low deposition rates. A typical deposition rate profile obtained [101] for the former system, at a deposition temperature of ~673 K, in a flow APCVD reactor, at a $C_2H_3Cl_2CH_3SiH_2$ consumption of 1.7×10^{-3} cm^3 s^{-1}, an oxygen consumption of 25 cm^3 s^{-1} and a gas mixture flow rate of 13 cm s^{-1}, was similar to the profile shown in Fig. 11 *a*; with a deposition rate in the order of 0.08 nm s^{-1}, this is two orders of magnitude lower than that for the oxidation of monosilane. The second system [102] exhibited a lowest practically admissible deposition rate of ~0.17 nm s^{-1}, only at temperatures above 823 K.

h. System $(C_2H_5O)_4Si-O_3/O_2$

The $(C_2H_5O)_4Si-O_3/O_2$ system has been widely used in electronic technologies since the mid-1990s. At relatively low deposition temperatures, the growth rate of silicon dioxide films is high, with a low level of side aerosol phenomena. In addition, the system exhibits a unique 'smoothed' character in its film growth on stepwise reliefs, which has found practical applications. Unfortunately, there is lack of comprehensive experimental studies of the kinetics of thin film growth in this system, in spite of the availability of much practically useful technological data.

Tetraethoxysilane has long been used as the starting compound in the deposition of silicon dioxide thin films; however, the information available mainly concerns the pyrolysis of TEOS.[102–106] This reaction proceeds at a noticeable rate at temperatures above 923 K (practically useful temperatures exceed 973 K); detailed consideration of the process being given below. It was also found[104] that in the presence of oxygen, the oxide thin films also grow at lower temperatures, and the maximum deposition rate is achieved at ~673 K (Fig. 27 *a*). It was assumed that this reaction results in the formation of polymeric structures.

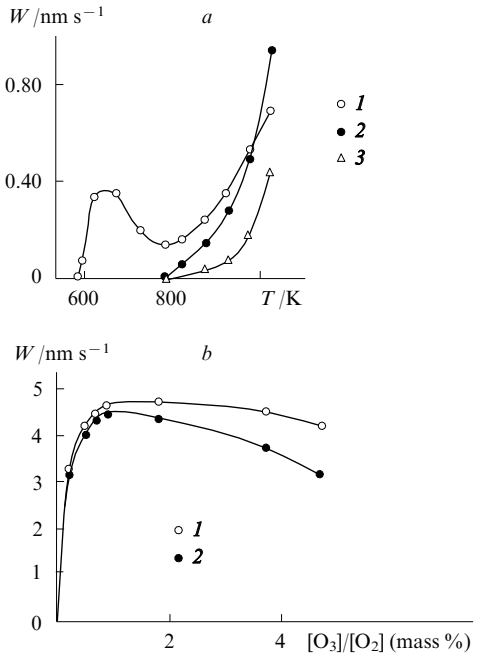


Figure 27. Thin-film deposition rate in the TEOS–O_2 (*1*), TEOS–H_2 (*2*) and TEOS–Ar (*3*) systems plotted *vs.* temperature (*a*) and the SiO_2 film deposition rate plotted *vs.* ozone concentration in the gas mixture for the silicon (*1*) and SiO_2 thermally grown on silicon (*2*) wafers (*b*).[107, 108]

Studies [107, 108] on the possibility of a substantial increase in the thin film deposition rate, using ozone–oxygen mixtures containing ~1 mass% of ozone as oxidants, for the low-temperature oxidation of TEOS (Fig. 27 *b*) were of great practical interest in the early 1990s. At higher absolute values of growth rate, the temperature dependence of the deposition rate in the presence of ozone retains its shape, shown in Fig. 27 *a* for the TEOS–O_2 system. However, in this case, a practically valuable increase in the growth rate is accompanied by non-stationarity of the film growth in the initial stage of the deposition reaction and by selectivity of thin film growth on the silicon, silicon dioxide and silicon nitride surfaces, which increases as the ozone concentration in the gas mixture increases. An increase in the deposition selectivity is accompanied by improved conformality of deposition and, as a consequence, by the appearance of a smoothed profile for deposited thin films on stepwise reliefs.[108]

The deposition of thin films in the TEOS–O_3/O_2 system can be considered as a new avenue in the CVD of oxide thin films, and of considerable research interest. However, most studies reported so far have been concerned with the practical aspects of CVD using a few types of industrial reactors. Not only the properties of silicon dioxide thin films, but also the film growth rate,[108–110] deposition selectivity, methods of controlling of this parameter using modified surfaces gas additives [111, 112] and the conformality of thin film deposition on stepwise reliefs, are the main parameters under study.[108–110, 113, 114]

In summarising the data on the growth rates for industrial processes of silicon dioxide thin film deposition at ~670 K and pressures of 25–100 kPa, with allowance for the fact that the

deposition rate is nearly first order with respect to TEOS and a pseudozero order with respect to O_3, the effective rate constant for the reaction was found to lie in the range 0.1–0.2 cm s^{-1}.

2. Pyrolysis reactions

Silicon dioxide, as well as Al_2O_3, SnO_2, TiO_2, ZrO_2, *etc.*, thin films can be grown by the pyrolysis of vapours of organoelement compounds;[9] SiO_2 deposition is mainly performed by pyrolysis of TEOS.[103–106] Industrial deposition processes of silicon dioxide thin films for electronics in isothermal flow LPCVD reactors[106] make it possible to fabricate films characterised by very low thickness uniformity ($\sim \pm 2\%$), simultaneously on a total of 150 silicon wafers with diameters of up to 300 mm, arranged at a distance of $\sim$5 mm from one another. At temperatures above 973 K, the rates of pyrolysis in the presence and absence of oxygen are nearly equal. Nevertheless, oxygen additives are usually used in order to minimise the concentrations of carbon-containing impurities in the deposited silicon dioxide thin film.

The kinetic data characterise the pyrolysis of TEOS as a heterogeneous reaction involving dissociative adsorption of TEOS in the initial stages. It was assumed that monomolecular decomposition can proceed at temperatures above 773 K. The stoichiometry of the pyrolysis reaction remains unknown, because the composition of the side reaction products (CO_2, CO, H_2, H_2O, C_2H_4, *etc.*) has not been exactly determined. The thin film growth rate at 998 K and a total pressure of 46.6 Pa, expressed through the partial pressure of TEOS (p_{TEOS}), is described by the equation:

$$W = \frac{k_1 p_{TEOS}^{0.5}}{1 + k_2 p_{TEOS}^{0.5}}.$$

The effective activation energy for the reaction is $\sim$194.4 kJ mol^{-1} at a total pressure of 33.3 Pa. The equation for the rate constant of pyrolysis (in s^{-1}) in an APCVD reactor at 1023–1148 K with N_2 as the medium takes the form:

$$k = 6.38 \times 10^{12} \exp\left(-\frac{238.2}{RT}\right).$$

3. Hydrolysis reactions

Vapour-phase hydrolysis of silicon, tin and titanium halides can be used to grow thin films of their corresponding dioxides at relatively low temperatures.[115–117] For instance, the interaction of SiF_4 with H_2O was studied at 753–858 K and gas mixture pressures lying in the range 11.9–93.3 kPa.[115] The growth kinetics of SnO_2 thin films was studied in the temperature range 753–981 K at linear flow rates exceeding 6 cm s^{-1} (in this case, mass transfer phenomena do not influence the reaction rate).[116] Fluorine-containing silicon dioxide thin films, which have a more complex composition, are fabricated by the hydrolysis of alkoxy halides $FSi(OAlk)_3$ at room temperature

$$FSi(OAlk)_3 + 3\,H_2O \longrightarrow FSi(OH)_3 + 3\,AlkOH$$

followed by polymerisation.[118]

The limited use of low-temperature hydrolysis reactions in high-precision technologies for the fabrication of silicon dioxide thin films is mainly due to the low quality of the films produced.

Hydrolysis of $AlCl_3$ and $SiCl_4$–$AlCl_3$ mixtures at temperatures above $\sim$1123 K in mixtures with CO_2 and H_2 is described by the following reactions:[119, 120]

$$H_2 + CO_2 \longrightarrow H_2O + CO,$$

$$2\,AlCl_3 + 3\,H_2O \longrightarrow Al_2O_3 + 6\,HCl,$$

$$SiCl_4 + 2\,H_2O \longrightarrow SiO_2 + 4\,HCl,$$

which eventually result in Al_2O_3 and SiO_2 or in alumosilicates (of general formula Al_2SiO_5) in co-hydrolysis of halides.

The formation of Al_2O_3 thin films was studied at a pressure of 13.3 kPa in the temperature range 1173–1423 K. The composition of the vapour phase (in mole fractions) was as follows: hydrogen, 0.05–0.95; $AlCl_3$, 0.005–0.03; CO_2, up to 100%.[119] Under these conditions, supersaturation with water vapours varied from 1.01 to 1.20 and supersaturation with $AlCl_3$ varied from 10^7 to 7.0×10^{11}. The kinetic data were obtained under the conditions where the thin film growth rate was independent of the gas flow rate. The reaction rate at 1300 K increased as the partial pressure of $AlCl_3$ increased, reached a maximum value at $\sim$133.3 Pa and then decreased on further increase in the partial pressure of $AlCl_3$. The dependence of the growth rate on the partial pressure of H_2 obeyed an identical pattern, with the maximum value reached at $\sim$7.33 kPa. The temperature dependence of the process was characterised by an activation energy of 146.3 kJ mol^{-1}. Most probably, the results obtained correspond to a heterogeneous reaction.

Co-hydrolysis of $SiCl_4$ and $AlCl_3$ was studied at temperatures 1123–1373 K, a pressure of 13.3 kPa, gas flow rates in the range 3.67–16.7 cm^3 s^{-1} and mole fractions of 0.006–0.05 for $SiCl_4$, 0–0.015 for $AlCl_3$ and 0.035–0.25 for CO_2.[120] The deposition rate of the films obtained at deposition temperatures above $\sim$1273 K under nearly optimum conditions was higher than $\sim 1.6 \times 10^{-4}$ mg cm^{-2} s^{-1}. The activation energy for the deposition of SiO_2, Al_2O_3 and alumosilicates at deposition temperatures above 1273 K was $\sim$83.6 kJ mol^{-1} and increased to $\sim$290 kJ mol^{-1} at lower temperatures for hydrolysis of SiO_2. The most interesting result obtained is a clearly seen linear dependence of the alumosilicate deposition rate on the mole fraction of $AlCl_3$ in the mixture, which considerably increases as the reaction temperature decreases; no dependence on the mole fraction of $SiCl_4$ in the studied range of the experimental conditions was observed.

4. Plasma-enhanced oxidation reactions

Fabrication of oxide thin films in the oxidation reactions carried out at low temperatures ($\sim$670 K) and pressures of several hundreds of Pa using plasma-enhanced gas mixtures is of paramount practical interest, being in fact a specific field of CVD research. Considerable literature on the subject is available (see, *e.g.*, Refs 4–6, 54–56, 121–124).

The first system used for plasma-enhanced deposition at $\sim$670 K was SiH_4–N_2O. Since the early 1990s the TEOS–O_2 system has been used. In principle, low-temperature plasma-enhanced synthesis of oxide films can also be performed using plasma-enhanced pyrolysis of organosilicon compounds (*e.g.*, TEOS, hexamethyldisiloxane, trimethoxychloromethylsilane, *etc.*) in an oxygen-free medium, because these molecules contain Si–O bonds.[54] However, the oxide films obtained contain a considerable amount of carbon, which is undesirable for microelectronic devices. In this connection a necessary condition for plasma-enhanced synthesis of oxide films of desired quality is the presence of oxidants. In this case, in accord with the equation

$$(C_2H_5O)_4Si + 12\,O_2 \longrightarrow SiO_2 + 10\,H_2O + 8\,CO_2$$

even at 12-fold excess of an oxidant with respect to TEOS, the content of carbon in the films obtained can be high (up to $\sim 3 \times 10^{20}$ atom cm^{-3}) and detectable by secondary ion mass spectrometry (SIMS). It was established that minimisation of the carbon content in the deposited films down to an admissible level of $\sim 0.3 \times 10^{20}$ atom cm^{-3} requires a 30–40-fold excess of oxygen with respect to TEOS.[125]

The deposition rate in the systems under study can be characterised as being first-order with respect to the source of silicon and a pseudozero order with respect to oxidant. The plot of the dependence of the deposition rate on the supplied high-frequency power is a curve with a linear portion followed by a plateau corresponding to the deposition. This permits variation of mechanical strain in the deposited film by varying the high-frequency power. (Optimisation of mechanical strain is of great importance for practical use of dielectric silicon dioxide thin films as passivators of metallisation of electronic devices). The activa-

tion energies for the plasma-enhanced oxidation reactions are ~ 10 kJ mol^{-1}, which suggests that the temperature has little effect on the film growth kinetics.

The effective rate constant for plasma oxidation CVD processes was estimated at $k_{ef} > 1$. By and large, plasma enhanced deposition processes of silicon-containing films are consistent with the classification of CVD processes given in Table 2 and obey the laws of film growth on stepwise reliefs.

5. Industrial methods of silicon dioxide film deposition

Depending on the deposition temperature, silicon dioxide films used in electronics are divided into medium-temperature films (920 – 1000 K) and low-temperature ones (~ 670 K); the latter being used for production of wafers containing metallic conductors. A commonly accepted medium-temperature method is oxidative pyrolysis of TEOS in isothermal LPCVD reactors. This industrial process has the best performance and parameters of deposited SiO_2 films including the conformality of film growth on complex-shape reliefs.

At present, the most widely used industrial low-temperature CVD methods are oxidation of monosilane by oxygen at an atmospheric or low pressure, plasma-enhanced oxidation of TEOS by oxygen and of monosilane by N_2O and oxidation of TEOS by an ozone – oxygen mixture at an atmospheric or reduced pressure. The last-mentioned method is of limited use because of the drawback of the low density of silicon dioxide films, which depends on the properties of the material subjected to deposition. Fast methods of silicon dioxide deposition including plasma-enhanced techniques are mainly used in order to grow films on plane wafers; films on wafers with a complex relief are fabricated using oxidation by ozone – oxygen mixtures.

Recently, very dense silicon dioxide thin films with the high-quality (continuous) filling of narrow (< 0.2 μm) gaps of a stepwise relief in microelectronic devices have been fabricated using the so-called 'high-density plasma' CVD (HDP-CVD) technique, where film deposition in the $SiH_4 - O_2$ system at pressures below 1 Pa is combined with sputtering of the material deposited by argon ions.[126] These processes have been comprehensively covered in Refs 32 and 33.

VII. Deposition of multicomponent silicate glass thin films

Multicomponent dielectric thin films based on glass-forming oxides SiO_2, P_2O_5, B_2O_3 and GeO_2, and belonging to silicate glasses, are prepared by CVD techniques and widely used in high-precision technologies as insulators.[3 – 6, 127, 128] Silicate glasses also possess specific properties, *e.g.*, the ability to help alkali metal ions, undergo a viscous flow at elevated temperatures, *etc*. Such glass films have long been used, but only a few kinetic studies of their growth characteristics are available. The reason for the lack of detailed kinetic studies is that such films were fabricated in industrial reactors only. To some extent this can be explained by the fact that the major component of practically interesting (valuable) compositions of silicate glasses is SiO_2 (the overall concentration of other oxides is, as a rule, at most 30 mass %). Because of this, the processes of chemical vapour deposition of glasses are usually studied by analysing the changes upon the introduction of the second, third, *etc*., components in the gas mixtures constituting the source of silicon and oxidant.

Binary phosphosilicate glass (PSG) and ternary borophosphosilicate glass (BPSG) films are best studied and most widely used in electronics.[28, 30, 31, 127 – 137] A necessary feature of glass film fabrication under the CVD conditions is the use of a strong oxidant. In the absence of the strong oxidant or when using a weak oxidant (*e.g.*, N_2O), it is impossible to fabricate glass films without the use of excess silicon and carbon and the phosphorus content in the films is at most 1 mass%. It is commonly accepted that the glass-forming oxides (SiO_2, B_2O_3 and P_2O_5) are formed as a result of independent oxidation reactions of hydrides SiH_4, PH_3 and B_2H_6, esters of silicic, boric, phosphorous and phosphoric acids and boron and phosphorus chlorides under the CVD conditions according to the schemes

$$4\,PH_3 + 5\,O_2 \longrightarrow 2\,P_2O_5 + 6\,H_2,$$

$$2\,B_2H_6 + 3\,O_2 \longrightarrow 2\,B_2O_3 + 6\,H_2.$$

However, exact equations of the oxidation reactions are unknown because the compositions of the side products depend on particular CVD conditions and have not been studied in detail (see above).

There are two main methods of fabrication of phosphorus- and boron-containing glass thin films, which are basic to industrial deposition techniques. One of them involves a combination of monosilane and hydrides, chlorides or organic esters at deposition temperatures in the range 620 – 720 K at atmospheric pressure or at low pressure of reagents. The other uses a combination of TEOS with phosphine or organic esters of boric, phosphorous or phosphoric acids and can be practically implemented in three versions, *viz*., at 920 – 100 K and low pressure, at ~ 673 K under PE-CVD conditions and at 670 – 770 K and atmospheric or reduced pressure of O_3/O_2 mixtures (ozone concentration varies from 4 mass % to 12 mass %). The characteristics of five main industrial CVD processes are listed in Table 6. All these methods can be used for fabrication of not only BPSG thin films with boron and phosphorus concentrations of up to ~ 6 mass % – 8 mass % with respect to each element but also silicon dioxide and binary glass films by appropriately combining the starting reagents.

By and large, the glass film deposition processes are similar. They are nearly first order reactions with respect to the silicon-containing compounds and proceed in the presence of a large excess of oxidants, which corresponds to a pseudozero order with respect to the oxidants. The activation energies for the CVD oxidation processes (except for plasma-enhanced processes) reported by different authors lie in the range 62 – 209 kJ mol^{-1}, those of the PE processes being an order of magnitude lower.

The influence of phosphorus- and boron-containing compounds on the parameters of the CVD processes of glass films is illustrated in Fig. 28 *a*. Here, the ratios of the deposition rates (W) of PSG and borosilicate glass (BSG) films to the deposition rate of silicon dioxide (W_{SiO_2}) are plotted *vs*. the change in the mole ratio of the boron or phosphorus compounds to the mole ratio of the silicon compound in the vapour phase.

In the presence of phosphorus-containing compounds the oxidation reactions of silicon compounds are accelerated and their activation energies appreciably decrease (by a factor of 1.3 – 3). Acceleration of the reactions is favoured by a proportional increase in the phosphorus content in the deposited PSG and BPSG films, by a decrease in the film thickness uniformity and by enhanced formation of aerosol side products. The greatest acceleration of the CVD of silicate glass films (from 3 to 7 times) is achieved when using a mixture of TEOS with PH_3 while the minimum acceleration is attained for the oxidation of monosilane mixed with any phosphorus compound mentioned above.

The oxidation reactions of monosilane, phosphine and other phosphorus compounds by dioxygen are known to proceed by a branched chain mechanism (see above). Taking into account this fact and the retardation of the oxidation reactions in the order $PH_3 - PCl_3 -$ organic esters, the acceleration of the oxidation CVD processes studied clearly indicates their branched chain mechanism. However, boron compounds cause the CVD processes involving monosilane and phosphine to slow down, *i.e*., inhibit the BCP. This is indicated by a decrease in the glass film deposition rate in the course of the oxidation processes involving monosilane and by a decrease in the phosphorus content in the glass films upon introduction of boron compounds into the starting gas mixtures. On the contrary, relatively slow TEOS oxidation reactions are accelerated upon introduction of boron compounds into the gas mixtures. The effect of the interaction

Table 6. Main characteristics of industrial glass film deposition processes.[30–32]

Characteristic or parameter	CVD technology				
	1	2	3	4 (PE-CVD)	5 (HDP-CVD)
Reactor type	see Fig. 4 a,*c*,*d*	see Fig. 4 *c*,*d*	see Fig. 4 *b*	see Fig. 4 *b*	see Ref. 6
Wafer diameter /mm	60, 76, 100	100, 150	150, 200	200	200
Deposition temperature /K	670–730	970–1130	710–770	650–690	650–890
Plasma enhancement	no	no	no	yes	yes
Silicon source	SiH_4	TEOS	TEOS	TEOS	SiH_4
Phosphorus and boron sources	PH_3 B_2H_6, esters	PH_3, PCl_3, esters	esters	esters	PH_3
Oxidant	O_2	O_2	O_3/O_2	O_2	O_2
Pressure /Pa	60–260	60–260	$(2–10)\times10^4$	665–1730	~0.6
Carrier gas	N_2/Ar	Ar	He	N_2	Ar
Growth rate /nm s^{-1}	~0.5–8 (APCVD reactor), ~0.08–0.25 (LPCVD reactor)	up to ~0.35	5–10	up to ~17	~7
Film thickness uniformity (±%)	<10	<3	<1.5	<2	<2
Effect of phosphorus compounds on the deposition process	acceleration	acceleration	acceleration	acceleration	–
Effect of boron compounds on the deposition process	retardation	acceleration	acceleration	acceleration	–
τ_{max} /s	⩽0.025	~0.05	~0.05	–	–
k_{ef} /cm s^{-1}	2.0–2.6	0.8–1.1	1.1–1.5	2–5	–
Surface roughness /nm	~12 (APCVD reactor), ~2.5 (LPCVD reactor)	–	~2.1 (APCVD reactor), ~0.9 (LPCVD reactor)	0.8	0.5
Conformality (h_2/h_1) (%)	30–40	60–80	60–80	10–30	–
Gap-fill test (h_{st}/G^2) /μm^{-1}	–	–	<4	<1	>20

between the boron and phosphorus compounds in the course of CVD processes on the final parameters of the deposited BPSG thin films can be characterised as follows: phosphorus compounds favour incorporation of boron into the film deposited while boron compounds inhibit the incorporation of phosphorus into the glass thin film.

A good illustration of the influence of acceleration and retardation of CVD processes is provided by Fig. 28 *b*. A model flow reactor is characterised by a generalised SiO_2 deposition rate profile (curve *3*) obtained by recalculating the experimental data to the corresponding coordinates. Analysis of the experimental profiles showed that the glass film deposition kinetics is governed by the phosphorus compounds. The presence of phosphorus compounds causes acceleration of the reactions and a shift of the deposition rate profiles to the left (towards shorter residence times) and favours the formation of aerosol reaction products. At the same time the presence of boron compounds causes retardation of the oxidation reactions and a shift of the deposition rate profile to the right; no aerosol particles are observed in this case (see Fig. 28 *b*). The limiting BPSG growth rates achieved in different deposition processes can be ~1.5–2 times higher than the growth rates listed in Table 6, which favours incorporation of microparticles into the glass films. The directions in which undesired aerosol effects in the deposition of BPSG thin films increase are shown by arrows in Fig. 28 *b*.

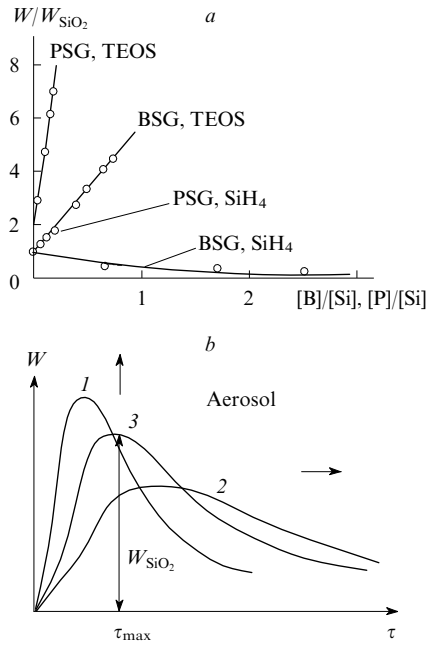


Figure 28. Effect of phosphorus- and boron-containing compounds on the parameters of CVD processes (*a*) and the influence of acceleration (*1*) and retardation (*2*) of the oxidation reaction on the shape of the deposition rate profile in a flow reactor (*3*) (*b*).[28,30] For details, see text.

A comparison of various oxidation processes used for glass film deposition showed that in the case of PSG and BPSG the k_{ef} value can lie in the range 1.1–2.5 cm s^{-1}. Thus, in spite of considerable differences between the deposition of SiO_2 films involving monosilane and TEOS, the kinetic characteristics of these processes are quite similar to those of the deposition processes of glass films of similar compositions.

The problem of the quality of the surfaces of films deposited is topical when one deals with the CVD of glass films involving BCP. The surface roughness of a glass film is characterised (naked-eye observation) using such terms as 'mirror', 'with inclusions', 'haze', *etc*. The kinetic data on the CVD of glasses can be checked by studying the surface roughness of the BPSG films obtained by different methods using atomic force microscopy.[138] This method has been used in the thin-film surface roughness measurements since the mid-1990s. Comparative studies of the surfaces of glass films of different compositions have revealed some trends.[138] For instance, acceleration of the oxidation reactions by phosphorus compounds makes the glass surfaces rougher while retardation of the same oxidation reactions by boron compounds reduces the surface roughness. The surface roughness of thin films fabricated from TEOS by the methods 3 and 4 (see Table 6) lies in the range

0.8–2 nm. This is on average nearly 2.5 (6) times lower than surface roughness of thin films fabricated from monosilane by the method 1 at atmospheric (low) pressure. This confirms the occurrence of intense vapour-phase processes in the course of CVD involving monosilane. The large difference between the surface roughness of the thin films prepared at low and atmospheric pressures can be explained by substantially different growth rates.

The surface roughness of BSG thin films is about twice lower than those of the PSG and BPSG thin films fabricated under similar conditions. This result clearly indicates a decrease in the intensity of vapour-phase reactions in the presence of boron-containing compounds in the gas mixture. The maximum surface roughness of silicon dioxide films prepared by the oxidation of TEOS by a O_3/O_2 mixture is ~ 6 nm. This value decreases by more than an order of magnitude upon introduction of esters of boric and phosphoric acids to the gas mixture; apparently, in this case the mechanism of the CVD process changes.

Acceleration and retardation of oxidation processes by phosphorus and boron compounds suggests that the oxidation of the gas mixture components involves formation of common intermediates rather than intermediate products of individual reactions. Although the mechanisms of the oxidation reactions proceeding in the course of BPSG fabrication have not been studied so far, the totality of kinetic data on the influence of phosphorus compounds unambiguously points to the similarity of the mechanisms of the PSG and BPSG film deposition reactions involving radicals formed in the interaction between phosphorus-containing compounds and oxidants. This was included in a generalised scheme of the synthesis of oxide films,[28,30] which is based on the concept of multistage and multipath processes of the growth of dielectric films under CVD conditions (see above).

A scheme of the deposition of silicon dioxide and glass films is presented in Fig. 29 (shown is an example of a multicomponent chemical reaction involving TEOS, for which the acceleration effect is most pronounced). Heterogeneous formation of silicon dioxide (route *I*) proceeds either as pyrolysis of TEOS on the surface at high temperatures or, in the presence of ozone, as a reaction of adsorbed TEOS and ozone at low temperatures. In the latter case the structure of the film deposited is rougher and more porous than the structure of silicon dioxide films fabricated using oxygen as oxidant. This indicates that the silicon dioxide films are more structurally ordered. If boron and phosphorus compounds are introduced in the gas mixture, the process follows a two-stage scheme (route *II*), which implies homogeneous formation of intermediate products I_X and I_Y involving phosphorus-containing radicals (asterisked) followed by heterogeneous transformation of I_X and I_Y into the film deposited on the wafer. In the case of PSG and BPSG, the film growth processes are limited by the stage of homogeneous formation of intermediate products I_X, whereas the growth of borosilicate glass films following the second route is limited by the heterogeneous stage of consumption of intermediate products I_Y. Aerosols are formed following route *III* involving formation of clusters (including those containing boron and phosphorus oxides) in the vapour phase.

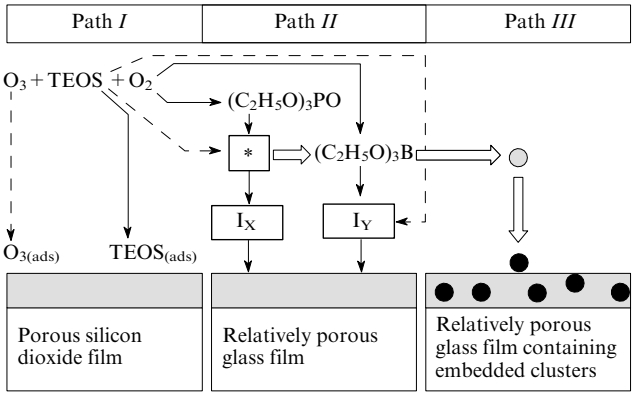


Figure 29. Three-path scheme of chemical vapour deposition of SiO_2 and glass films in a chemical system containing organic esters of silicic, boric and phosphoric acids.[28,132]

A characteristic feature of glassy materials obtained from organic esters is the presence of carbon impurities in the films deposited. For instance, SIMS studies of phosphorus-enriched films prepared by the method 3 (7 mass % of phosphorus and 3 mass % of boron) revealed a uniform distribution of carbon along the film thickness and showed that its content is nearly three times lower than in the films with a similar content of phosphorus (4 mass %) and boron (4.5 mass %), being $\sim 1.05 \times 10^{19}$ and $\sim 3.19 \times 10^{19}$ atom cm^{-3}, respectively. Hydrogen impurities are present in glasses obtained by all deposition techniques. Generally, the content of hydrogen increases if the CVD temperature is below 670 K. The PSG and BPSG thin films freshly deposited by the method 3 and containing 4 mass% of boron and phosphorus are characterised by uniform distribution of hydrogen, its initial content being equal to $\sim 3 \times 10^{20}$ atom cm^{-3}. The content of hydrogen in the glass films prepared by the methods 4 and 5 is $\sim 6 \times 10^{20}$ and $\sim 4 \times 10^{20}$ atom cm^{-3}, respectively.

Because of multicomponent composition of silicate glasses, many factors must be controlled. Among them, the most important is the behaviour of the phosphorus and boron components of the glass. Their concentrations and uniformity of distribution across the surfaces of wafers are determined either using destructive methods of spectral analysis, dissolution, *etc.*, or by pre-calibrated non-destructive methods (IR spectroscopy and X-ray fluorescence).

The compositions of the glass thin films prepared by CVD in the presence of a large excess of oxidants are similar to the compositions of stoichiometric glasses, *i.e.*, the films contain silicon, boron and phosphorus oxides SiO_2, B_2O_3 and P_2O_5, respectively. The absence of excess silicon is indicated by the refractive index values of these thin films (from 1.44 to 1.48) measured by ellipsometry. Phosphorus-containing compounds are oxidised to P_2O_5; however, in some cases ion chromatography of glasses reveals the presence (less than ~ 1 mass %) of phosphorus in the oxidation state $+3$, which corresponds to the phosphorus oxide P_2O_3. This is characteristic of the low-temperature processes of PSG and BPSG deposition from hydrides at low pressure and of the plasma-enhanced deposition techniques involving phosphines under oxidant-deficient conditions (or in the presence of a weak oxidant) at considerable high-frequency power supplied. For the plasma-enhanced glass deposition techniques, it was also reported that the ESCA spectra revealed the formation of not only the P–O (134 eV) but also the Si–P (130 eV) bond. Only phosphorus in the oxidation state $+5$ is detected in the thin films prepared using the oxidation systems involving organic esters at large excesses of oxidants. No phosphorus in other oxidation states was detected in the PSG thin films deposited in high-density plasma involving hydrides.[139] The use of appropriate synthetic strategy leads to uniform distribution of boron and phosphorus along the thickness of different BPSG thin films; this was confirmed by the results of layer-by-layer SIMS analysis.

Silicate glass thin films possess different properties. First of all, such films differ in degree of structural imperfection (defectness). One must distinguish between two components of this parameter. One component characterises the deposition technique itself (*i.e.*, the state of the equipment and the extent of optimisation of the deposition conditions) and is measured immediately after the deposition. The second component characterises the degree of defect of glasses as a specific property of the glassy material (*e.g.*, BPSG) and manifests itself when the glass film is exposed to atmospheric air. Depending on the glass composition, the value of this component can increase by several orders of

magnitude over short time intervals.[134] Problems concerned with the defectness of glass films are summarised in Refs 31 and 133–135.

Different properties of the glass thin films were explained by their different compositions and structures due to the use of a variety of deposition methods. The structure of the BPSG thin films is first of all determined by the boron-to-phosphorus oxide ratio in the glass. The dependence of the reactivity of the BPSG thin films towards, *e.g.*, absorbed water vapours $H_2O_{(abs)}$ present in the air on the film composition can be explained by the presence of boron atoms coordinated to three oxygen atoms (BO_3) in the glass network, in which the silicon and phosphorus oxides are present in the form of tetrahedral SiO_4 and PO_4 units. The glass structural fragments $(\equiv Si-O-)_3OP$ and $(\equiv Si-O-)_3B$ react with water vapour as follows:

$$(\equiv Si-O-)_3OP + H_2O_{(abs)} \longrightarrow \equiv Si-OH + (\equiv Si-O-)_2OPOH,$$

$$(\equiv Si-O-)_3B + H_2O_{(abs)} \longrightarrow \equiv Si-OH + (\equiv Si-O-)_2BOH.$$

Prolonged interaction between the glass and water vapour and replacement of $\equiv Si-O-$ groups by $-OH$ groups lead to gradual leaching of boron and phosphorus from the glass film and formation of droplets containing phosphoric and boric acids on the glass surface. It was shown that the content of boron atoms coordinated to three oxygen atoms decreases with an increase in the concentration of phosphorus oxide in the glass film and that the content of boron atoms coordinated to four oxygen atoms increases. As a result, an increase in the phosphorus-to-boron content ratio in the glass makes the material less reactive towards water vapour in air.

Interrelation between the properties of glasses and specific features of deposition processes can be explained as follows. The most important physical property of glass thin films is their effective density (or its reciprocal, porosity). Unfortunately, no data on the density of the BPSG thin films, measured by direct methods are available in the literature as yet. Based on the totality of data on, in particular, the shrinkage and etch rates of samples in aqueous solutions of hydrofluoric acid, the highest porosity was ascribed to silicon dioxide, PSG, BSG and BPSG thin films fabricated by low-temperature oxidation of organic esters by O_3/O_2 following the method 3 (see Table 6). The lowest porosity was ascribed to the thin films of the same glasses, fabricated by the PE-CVD (method 4) and especially the HDP-CVD (method 5) techniques. The highest porosity of the SiO_2 and BSG thin films fabricated using the method 3 is associated with low k_{ef} value. This process was described in the framework of the two-stage scheme of sequential reactions with the heterogeneous limiting stage involving consumption of intermediate products, which is responsible for the formation of disordered glass structures in the course of the CVD process. On the contrary, fast deposition processes described in the framework of the two-stage scheme of sequential reactions with the homogeneous limiting stage involving formation of intermediate products make it possible to grow much more ordered (*i.e.*, dense) thin films.

VIII. Conclusion

The authors of this review presented the key information on the chemical vapour deposition of layered dielectric materials and on the properties of covalent dielectrics used in electronics. Layered dielectric composites can be used not only in high-precision technologies but also in mechanical engineering, power engineering, medicine, *etc.*, the CVD methods are considered to be quite promising because they provide unique possibilities of deposition of thin and ultrathin coatings with preset properties and high mechanical and adhesive characteristics on surfaces with complex-shape reliefs.

Chemical transformations of reagents on the surface of a growing layer in the course of the CVD process occur within a layer that is somewhat thicker than a monolayer. This is basic to the definition of the reaction zone concept. For different CVD processes, the thickness of the reaction zone can vary between a few and several tens of Ångströms. Because of the lack of reliable information on the structure of the reaction zone, researchers are forced to employ a traditionally used description of heterogeneous processes, which is based on the concept of an ideal adsorption layer (Langmuir–Hinshelwood or Ealey–Rideal kinetics), which uses physically incorrect models. Further progress in the CVD methods is closely related to the studies on the structure and dynamics of the reaction zone, which govern not only the dynamics and kinetics of the processes but also the main characteristics of the growing layer. Advances in solving the problems considered above are to a great extent due to the use of modern experimental equipment and especially the *in situ* recording techniques used in the course of the CVD processes. These are, *e.g.*, automatic ellipsometry and piezoquartz microbalance methods, which allow the dynamics and (under steady-state conditions) the kinetics of the process to be investigated. The laser heating technique (chemical thermometer) permits separation of the contribution of pure vapour-phase stages while the IR and Raman spectroscopies provide the possibility of monitoring the composition and temperature of the reacting gas flow. Modern methods of investigation of the aerosol phase make it possible to study nucleation in the vapour phase and to control the structural homogeneity of the deposited coatings.

References

1. C F Powell, J H Oxley, J M Blocher Jr. (Eds), in *Vapor Deposition* (New York: Wiley, 19870)
2. G Hass, R E Tun (Eds) *Physics of Thin Films* (New York, London: Academic Press, 1967)
3. W Kern, V S Ban, in *Thin Film Processes* (Eds J L Vossen, W Kern) (New York: Academic Press, 1978) p. 257
4. A C Adams, in *VLSI Technology* (Ed. S M Sze) (New York: McGrow-Hill, 1988) p. 223
5. S Wolf, R Tauber *Silicon Processing for VLSI Era* Vol. 1 (Sunset Beach: Lattice Press, 1986)
6. H C Cheng, in *ULSI Technology* (Eds C Y Chang, S M Sze) (New York: McGrow-Hill, 1996) p. 205
7. L L Vasil'eva, in *Sovremennye Problemy Fizicheskoi Khimii Poverkhnosti Poluprovodnikov* (Modern Problems of the Physical Chemistry of Semiconductor Surface) (Eds A V Rzhanov, S M Repinsky) (Novosibirsk: Nauka, 1988) p. 152
8. A V Rzhanov (Ed.) *Nitrid Kremniya v Elektronike* (Silicon Nitride in Electronics) (Novosibirsk: Nauka, 1982)
9. G A Razuvaev, B G Gribov, G A Domrachev, B A Solomatin *Metalloorganicheskie Soedineniya v Elektronike* (Organometallic Compounds in Electronics) (Moscow: Nauka, 1972)
10. M Volmer *Kinetik der Phasenbildung* (Leipzig, Drezden: Theodor Steinkopff, 1939)
11. H Schäfer *Chemische Transportreaktionen* (Weinheim: Verlag Chemie, 1961)
12. F A Kuznetsov, G A Kokovin, Ya M Buzhdan *Izv. Sib. Otd. Akad. Nauk, Ser. Khim. Nauk* **2** 5 (1975)
13. R A Laudise *The Growth of Single Crystals* (Englewood Cliffs, NJ: Prentice-Hall, 1970); R L Parker *Crystal Growth Mechanisms: Energetics, Kinetics and Transport* (New York: Academic Press, 1970)
14. V K Leko, O V Mazurin *Svoistva Kvartsevogo Stekla* (The Properties of Quartz Glass) (Leningrad: Nauka, 1985)
15. R K Iler *The Chemistry of Silica* Vol. 2 (New York: Wiley-Interscience, 1979)
16. M Nogami, Y Moriya *J. Non-Cryst. Solids* **37** 191 (1980)
17. S S Lin *J. Electrochem. Soc.* **125** 1877 (1978)
18. S M Repinsky, in *Sovremennye Problemy Fizicheskoi Khimii Poverkhnosti Poluprovodnikov* (Modern Problems of the Physical Chemistry of Semiconductor Surface) (Eds A V Rzhanov, S M Repinsky) (Novosibirsk: Nauka, 1988) p. 90
19. S M Repinsky *Khim. Fiz.* **11** 1383 (1992) [a]

20. R L Myuller, in *Khimiya Tverdogo Tela* (Solid State Chemistry) (Leningrad: Leningrad State University, 1965) p. 9
21. A G Revesz *Phys. Status Solidi, A* **57** 657 (1980)
22. V A Radtsig, V A Khalif *Kinet. Katal.* **20** 705 (1979) [b]
23. V F Kiselev *Poverkhnostnye Yavleniya v Poluprovodnikakh i Dielektrikakh* (Surface Effects in Semiconductors and Dielectrics) (Moscow: Nauka, 1970)
24. H H Dunken, V I Lygin *Quantenchemie der Adsorption an Festkörperoberflächen* (Leipzig: VEB Deutscher Verlag für Grundstoffinduestrie, 1978)
25. V Yu Vasilev, M S Sukhov *Obzory po Elektronnoi Tekhnike. Ser. 7* (Reviews on Electronic Engineering, Series 7) Vol. 3–4 (Moscow: TsNII Elektronika, 1985)
26. V Yu Vasilev *Khim. Fiz.* **11** 1406 (1992) [a]
27. V Yu Vasilev *Mikroelektronika* **28** 175 (1999) [c]
28. V Yu Vassiliev, J Z Zheng, S K Tang, W Lu, J Hua, Y S Lin *J. Electrochem. Soc.* **146** 3039 (1999)
29. V Yu Vasilev *Mikroelektronika* **28** 183 (1999) [c]
30. V Yu Vasilev, Doctoral Thesis in Chemical Sciences, Institute of Solid State Chemistry and Mechanochemistry, Siberian Branch of the Russian Academy of Sciences, Novosibirsk, 2002
31. V Yu Vassiliev *J. Electrochem. Soc.* **150** F211 (2003)
32. V Yu Vassiliev, J L Sudijono, A Cuthbertson *Solid State Technol.* **44** 129 (2001)
33. V Yu Vasilev *Mikroelektronika* **31** 263 (2002) [c]
34. C E Morosanu *Thin Solid Films* **65** 171 (1980)
35. J N Purnell, R Walsh *Proc. R. Soc. London, Ser. A* **293** 543 (1966)
36. G Schulze, M Henzler *Surf. Sci.* **124** 336 (1983)
37. Ch Kleint, B Hartmann, H Z Meyer *Z. Phys. Chem.* **250** 315 (1972)
38. G A Vompe *Zh. Fiz. Khim.* **47** 1269 (1973) [d]
39. V V Nosov, S M Repinsky, F N Dul'tsev *Kinet. Katal.* **25** 530 (1984) [b]
40. S M Repinsky, L V Mironova *Izv. Sib. Otd. Akad. Nauk, Ser. Khim. Nauk* **2** 44 (1975)
41. T N Bell, K A Perkins, P G Perkins *J. Chem. Soc., Faraday Trans. 1* **77** 1779 (1981)
42. O I Semenova, L A Nenasheva, S M Repinsky *Izv. Akad. Nauk SSSR, Neorg. Mater.* **20** 791 (1984) [e]
43. V Yu Vasilev, L L Vasilyeva *Izv. Sib. Otd. Akad. Nauk, Ser. Khim. Nauk* **14** 86 (1983)
44. O I Semenova L A Nenasheva *Izv. Aksd. Nauk SSSR, Neorg. Mater.* **25** 56 (1989) [e]
45. R S Rosler *Solid State Technol.* **20** 63 (1977)
46. T A Brown, I J Kamins *Solid State Technol.* **22** 51 (1979)
47. M Praiteur, J Goldman *Semicond. Int.* **7** 250 (1984)
48. V Yu Vasilev, S M Maroshina *Elektron. Promst'* **10** 60 (1986)
49. V Yu Vasilev, S M Maroshina *Izv. Aksd. Nauk SSSR, Neorg. Mater.* **25** 600 (1989) [e]
50. V Yu Vasilev, S M Maroshina, in *Poluprovodnikovaya Mikroelektronika* (Ed. V S Shadrin) (Semiconductor Microelectronics) (Novosibirsk: Izd. NETI, 1989) p. 62
51. S E Morosanu, D Iosif, E Segal *Thin Solid Films* **92** 334 (1982)
52. K F Roenigk, K P Jensen *J. Electrochem. Soc.* **134** 1777 (1987)
53. A A Korkin, J V Cole, D Sengupta, J B Adams *J. Electrochem. Soc.* **146** 4203 (1999)
54. S N Shepelev, V Yu Vasilev, V P Popov *Obzory po Elektronnoi Tekhnike, Ser. 7* (Reviews on Electronic Engineering, Series 7) (Moscow: TsNII Elektronika, 1988) No. 7
55. J W Lee, K D Mackenzie, D Johnson, J N Sasserath, S J Pearton, F J Ren *Electrochem. Soc.* **147** 1481 (2000)
56. T P Smirnova, in *Problemy Elektronnogo Materialovedeniya* (Problems of Electronic Materials Science) (Ed. F A Kuznetsov) (Novosibirsk: Nauka, 1986) p. 61
57. A K Gaind, E W Hearn *J. Electrochem. Soc.* **125** 139 (1978)
58. P S Shantarovich *Acta Phisicochim. USSR* **2** 633 (1935)
59. C Cobianu, C Pavelescu *Thin Solid Films* **102** 361 (1983)
60. C Pavelescu, C Cobianu, L Condriuc, E Segal *Thin Solid Films* **114** 291 (1984)
61. L L Vasilyeva, V N Drozdov, in *Problemy Fizicheskoi Khimii Poverkhnosti Poluprovodnikov* (Problems of Physical Chemistry of Semiconductor Surface) (Ed. A V Rzhanov) (Novosibirsk: Nauka, 1978) p. 155
62. V V Azatyan, R G Aivazyan, L L Vasilyeva L A Nenasheva, S N Nesterova *Kinet. Katal.* **25** 1033 (1984) [b]
63. V V Azatyan, L L Vasilyeva, L A Nenasheva, S N Nesterova *Kinet. Katal.* **28** 1068 (1987) [b]
64. V V Azatyan *Usp. Khim.* **54** 33 (1985) [*Russ. Chem. Rev.* **54** 21 (1985)]
65. V V Azatyan, V A Kalkanov, A A Shavard *React. Kinet. Catal. Lett.* **15** 367 (1980)
66. V V Azatyan, V A Kalkanov, A A Shavard *Kinet. Katal.* **26** 1292 (1985) [b]
67. S A Harutunyan, T G Mkryan, E N Sarkisyan *Oxid. Commun.* **7** 49 (1984)
68. V R Brain, L N Krasnoperov, V N Panlilov *Oxid. Commun.* **6** 259 (1984)
69. R Withnall, L Andrews *J. Am. Chem. Soc.* **107** 2567 (1985)
70. T Kudo, S Nagase *J. Am. Chem. Soc.* **107** 2589 (1985)
71. T Kudo, S Nagase *J. Phys. Chem.* **88** 2833 (1984)
72. L C Snyer, K Raghavachari *J. Chem. Phys.* **80** 5076 (1984)
73. N K Serdyuk, V P Strunin, V N Panfilov *React. Kinet. Catal. Lett.* **29** 9 (1985)
74. F Kaufman *Prog. React. Kinet.* **1** 3 (1961)
75. A Shintani *J. Electrochem. Soc.* **124** 1771 (1977)
76. A Shintani *J. Electrochem. Soc.* **127** 426 (1980)
77. E Whitby, M Hashino *J. Electrochem. Soc.* **143** 3397 (1996)
78. L L Vasilyeva, L A Nenasheva, V V Nosov *Khim. Fiz.* **11** 1399 (1992) [a]
79. L L Vasilyeva, V N Kruchinin, L A Nenasheva, V V Nosov *Poverkhnost'* **12** 54 (1992)
80. M R Baklanov, L L Vasilyeva, F N Dulcev *Thin Solid Films* **171** 43 (1989)
81. L L Vasilyeva, L A Nenasheva, V V Nosov *Kinet. Katal.* **33** 1059 (1992) [b]
82. F N Dultsev, L A Nenasheva, L L Vasilyeva *J. Electrochem. Soc.* **145** 2569 (1998)
83. T Takahashi, K Hagiwara, Y Egashira, H Komiyama *J. Electrochem. Soc.* **143** 1365 (1996)
84. T Takahashi, K Hagiwara, H Komiyama, Y Egashira *J. Electrochem. Soc.* **145** 1171 (1998)
85. A A Onishchuk, V N Panfilov *Usp. Khim.* **70** 368 (2001) [*Russ. Chem. Rev.* **70** 321 (2001)]
86. M S Sukhov, T 3 Shcheglova *Poverkhnost'* **4** 72 (1985)
87. M L Hitchman, J Kane *J. Cryst. Growth* **55** 485 (1981)
88. M L Hitchman, A E Widmer *J. Cryst. Growth* **55** 501 (1981)
89. L L Vasilyeva, L I Rabinovich *Izv. Sib. Otd. Akad. Nauk, Ser. Khim. Nauk* **9** 65 (1981)
90. L L Vasilyeva, S N Nesterova *Kinet. Katal.* **25** 1064 (1984) [b]
91. V Yu Vasilev, A N Kurchenko, in *Poluprovodnikovaya Tenzometriya* (Semiconductor Strain Measurement) (Ed. V S Shadrin) (Novosibirsk: Izd. NETI, 1988) p. 11
92. J G Wilkes *J. Cryst. Growth* **70** 271 (1984)
93. M Nishijima, H Kobayashi, K Edamoto, M Onchi *Surf. Sci.* **137** 473 (1984)
94. D-R He, F W Smith *Surf. Sci.* **154** 347 (1985)
95. R S Swann, A E Pyne *J. Electrochem. Soc.* **116** 1014 (1969)
96. W J Kroll, R L Titus, J Wagner *J. Electrochem. Soc.* **122** 573 (1975)
97. C D Dobson, A Kiermasz, K Beekman, R J Bilby *Semicond. Int.* **17** 85 (1994)
98. V Yu Vasilev, in *Poluprovodnikovaya Tenzometriya. Fizicheskie i Tekhnologicheskie Problemy* (Semiconductor Strain Measurement. Physical and Technological Problems) (Ed. V S Shadrin) (Novosibirsk: Izd. NETI, 1986) p. 70
99. W R Sinclair, J V Macchesney, P K Gallagher, P B O'Connor *Thermochim. Acta* **30** 225 (1979)
100. D L Wood, J V Macchesney, J P Luongo *J. Mater. Sci.* **13** 1761 (1978)
101. V Yu Vasilev, Candidate Thesis in Chemical Sciences, Institute of Solid State Chemistry and Mechanochemistry, Siberian Branch, Academy of Sciences of the USSR, Novosibirsk, 1990
102. C Smolinsky, R Dean *Mater. Lett.* **4** 256 (1984)
103. Yu S Dement'ev, A G Petrik, V P Tokarev *Zh. Fiz. Khim.* **48** 588 (1974) [d]
104. R P Kalnynya, I A Feltyn', L A Freiberg, I E Eglitis *Izv. Akad. Nauk SSSR, Neorg. Mater.* **5** 1540 (1969) [e]

105. A S Adams, S D Capio *J. Electrochem. Soc.* **126** 1042 (1979)
106. F S Becker, D Pawlik, H Anzinger, A Spitzer *J. Vac. Sci. Technol., B* **5** 1555 (1987)
107. K Fujono, Y Nishimoto, N Tokumasu, K Maeda *J. Electrochem. Soc.* **137** 2883 (1990)
108. K Maeda, S M Fisher *Solid State Technol.* **36** 83 (1993)
109. M D Dobkin, S Makhtari, M Schmidt, A Pant, L Robinson *J. Electrochem. Soc.* **142** 2332 (1995)
110. L-Q Xia, S Nemani, M Galiano, S Pichai, S Chandran, E Yieh, D Cote, R Conti, D Restano, D Többen *J. Electrochem. Soc.* **146** 1181 (1999)
111. K Tsukamoto, D Cheng, H Komiyama, Y Nishimoto, N Tokumasu, K Maeda *Electrochem. Solid State Lett.* **2** 24 (1999)
112. K Ikeda, S Nakayama, M Maeda *J. Electrochem. Soc.* **142** 1659 (1995)
113. K Ikeda, S Nakayama, M Maeda *J. Electrochem. Soc.* **143** 1715 (1996)
114. M Yoshimaru, T Yashie *J. Electrochem. Soc.* **145** 2847 (1998)
115. V A Arslambekov, K M Gorbunova, V I Karataeva *Izv. Akad. Nauk SSSR, Neorg. Mater.* **6** 1625 (1970) [e]
116. R N Ghoshtagere *J. Electrochem. Soc.* **125** 110 (1978)
117. K S Yeung, Y W Lam *Thin Solid Films* **109** 169 (1983)
118. T Homma *J. Electrochem. Soc.* **143** 707 (1996)
119. J-G Kim, C-S Park, J S Chun *Thin Solid Films* **97** 97 (1982)
120. S F Nitodas, S V Sotirchos *J. Electrochem. Soc.* **147** 1050 (2000)
121. J R Hollahan, R S Rosler, in *Thin Film Processes* (Eds J L Vossen, W Kern) (New York: Academic Press, 1978) p. 335
122. A K Adams *Solid State Technol.* **26** 135 (1983)
123. D W Hess *J. Vac. Sci. Technol., A* **2** 244 (1984)
124. D L Tolliver, in *VLSI Microelectronics Microstructure Science* Vol. 8 (Ed. N G Einspruch) (New York: Academic Press, 1984) p. 2
125. B J Schravendijk, D Carl, F Nagy, W Hoek, in *Proceedings of the 1st International Dielectric for ULSI Multilevel Interconnection Conference, Santa Clara, 1995* p. 141
126. M Sato, A Yoshinobu *J. Appl. Phys.* **256** L764 (1986)
127. R A Levy, K Nassau *J. Electrochem. Soc.* **132** 409 (1985)
128. T G Dukhanova, V Yu Vasilev, Yu I Veretenin *Obzory po Elektronnoi Tekhnike, Ser. 3* (Reviews on Electronic Engineering, Series 3) (Moscow: TsNII Elektronika, 1988) No. 4
129. V Yu Vasilev, T G Dukhanova *Khim. Fiz.* **11** 1699 (1992) [a]
130. S M Fisher, H Chino, K Maeda, Y Nishimoto *Solid State Technol.* **36** 55 (1993)
131. V Yu Vasilev *Zh. Fiz. Khim.* **73** 1191 (1999) [d]
132. V Yu Vasilev *Zh. Fiz. Khim.* **73** 1351 (1999) [d]
133. V Yu Vasilev *Fiz. Khim. Stekla* **26** 116 (2000) [f]
134. V Yu Vasilev *Fiz. Khim. Stekla* **26** 130 (2000) [f]
135. V Yu Vasilev *Fiz. Khim. Stekla* **29** 640 (2003) [f]
136. V Yu Vassiliev, C Lin, D Fung, J Hsieh, J L Sudijono *Electrochem. Solid State Lett.* **3** 80 (2000)
137. D L Simpson, R T Crosswell, A Reisman, C K Williams, D Tempie *J. Electrochem. Soc.* **147** 1560 (2000)
138. S K Tang, V Yu Vassiliev, S Mridha, L Chan *Thin Solid Films* **352** 77 (1999)
139. M C Hughes, D R Wonsidler *J. Electrochem. Soc.* **134** 1488 (1987)

[a] — *Chem. Phys. Rep. (Engl. Transl.)*
[b] — *Kinet. Catal. (Engl. Transl.)*
[c] — *Russ. Microelectron. (Engl. Transl.)*
[d] — *Russ. J. Phys. Chem. (Engl. Transl.)*
[e] — *Inorg. Mater. (Engl. Transl.)*
[f] — *Glass Phys. Chem. (Engl. Transl.)*